Geol. Mag. **145** (*3*), *2008, pp. 321–344. © 2007 Cambridge University Press*
doi:10.1017/S0016756807004244 *Printed in the United Kingdom*

Integrated stratigraphy and palaeoecology of the Lower and Middle Miocene of the Porcupine Basin

STEPHEN LOUWYE*†, ANNELEEN FOUBERT‡, KENNETH MERTENS*, DAVID VAN ROOIJ‡ & THE IODP EXPEDITION 307 SCIENTIFIC PARTY

*Research Unit Palaeontology, Ghent University, Krijgslaan 281/S8, 9000 Ghent, Belgium
‡Renard Centre for Marine Geology, Ghent University, Krijgslaan 281/S8, 9000 Ghent, Belgium

(*Received* 5 February 2007; *accepted* 26 June 2007; First published online 20 December 2007)

Abstract – A high-resolution palynological analysis and a detailed palaeomagnetic study of a marine sequence recovered during IODP Expedition Leg 307 in the Porcupine Basin southwest of Ireland provide new insights into the regional depositional history and palaeoenvironmental evolution during Early Neogene times. The Hole 1318B studied was drilled on the upper slope of the continental margin in a water depth of 409 m, upslope from a province of carbonate mounds (the Belgica mound province). The diverse and well-preserved dinoflagellate cyst associations consist typically of deep neritic and oceanic species, mixed with a neritic component transported from the shelf, reflecting the deep depositional setting at the continental margin. The palaeomagnetic record together with the ranges of key dinoflagellate cyst species constrain the age of the studied sequence between 16.7 Ma and 12.01 Ma, that is, between the late Burdigalian and late Serravallian. The distinct unconformity terminating the Miocene sequence correlates to the global sequence boundary Ser4/Tor1 dated at 10.5 Ma, and represents, according to previous extensive seismic studies, a basin-wide erosional event. The overlying sediments are of Middle Pleistocene or younger age. Downslope from IODP Site 1318, carbonate mounds root on the erosional surface. The dinoflagellate cyst associations from the Porcupine Basin distinctly mirror the global cooling phase following the Middle Miocene Climatic Optimum. Cooling phase Mi3, a short-lived glaciation, is particularly well expressed and here dated at 13.6 Ma. The palynomorph record furthermore indicates a reduction of the productivity and an increase of oceanic oligotrophic species after 14 Ma, suggesting a reduction or perhaps even a shutdown of the upwelling.

Keywords: Porcupine Basin, dinoflagellate cysts, magnetostratigraphy, palaeoenvironment, Miocene, IODP Expedition 307.

1. Introduction

The Porcupine Seabight (Fig. 1) initially gained fame at the end of the nineteenth century for its special deep-water habitats (Thomson, 1873; Le Danois, 1948). Hovland, Croker & Martin (1994) were the first to publish seismic profiles picturing mound structures up to 200 m high and more than 1500 m long. Very-high-resolution seismic profiling has confirmed the presence of large seabed (carbonate) mounds in the Porcupine Basin (Henriet *et al*. 1998; De Mol *et al*. 2002; Huvenne, Croker & Henriet, 2002). The mounds occur in three well-delineated provinces, featuring distinct morphologies: the Belgica mounds on the eastern flank (De Mol *et al.* 2002; Van Rooij *et al*. 2003), the Hovland mounds in the north (Hovland, Croker & Martin, 1994; De Mol *et al.* 2002) and a large number of buried Magellan mounds further to the northwest (Huvenne, Croker & Henriet, 2002; V. Huvenne, unpub. Ph.D. thesis, Ghent Univ. 2003). The mounds have been defined as deep-water coral banks where colonies of dead and living corals (namely *Lophelia pertusa* and *Madrepora oculata*) interact with sediment drifts in a dynamic environment (De Mol *et al*. 2002; Foubert *et al*. 2005). According to De Mol *et al.* (2002) and Van Rooij *et al.* (2003), mound growth probably started during Pliocene times after periods of erosion or non-deposition. The mounds reach heights of up to 250 m and widths of up to 5 km and are enclosed by sediment drifts (De Mol *et al*. 2002; Huvenne, Croker & Henriet, 2002; Van Rooij *et al*. 2003). Despite the diverse and large seismic datasets gathered over more than 20 cruises during the last decade, the knowledge of the internal structures, the initiation and growth of these impressive sea-floor features within the Porcupine Seabight and their interaction with sedimentary processes occurring along the continental margins remained elusive. During Integrated Ocean Drilling Program Expedition 307 in May 2005 aboard the *JOIDES Resolution,* Challenger mound, a prominent mound structure covered with dead cold-water coral rubble in the Belgica mound province, was drilled

†Author for correspondence: Stephen.Louwye@UGent.be

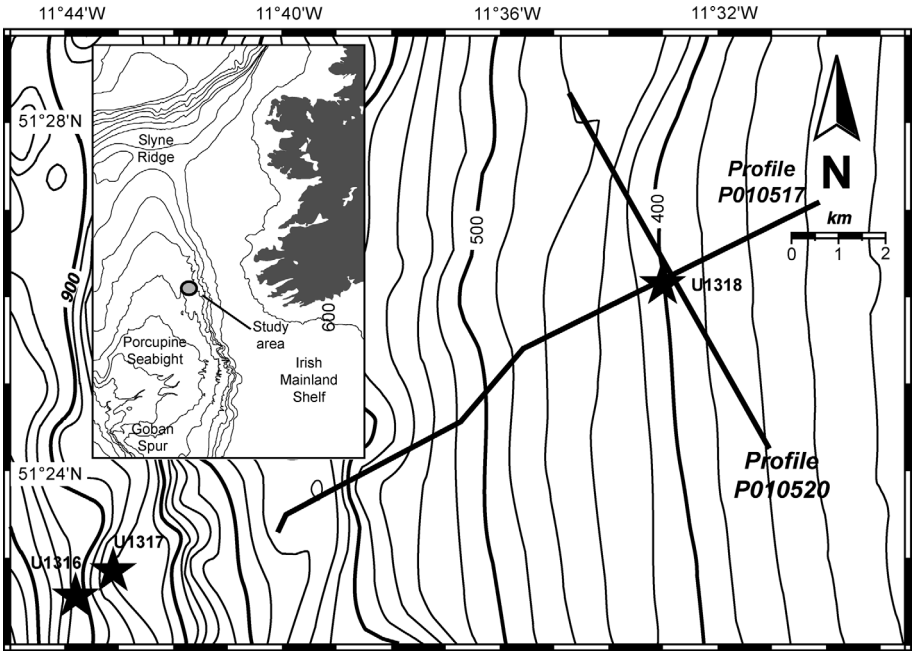

Figure 1. Location of drill sites IODP 1318A, 1318B and 1318C. Inset: location of the Porcupine seabight.

to the moundbase to unveil the internal structure of the mounds in Porcupine Seabight (Site U1317, Fig. 1). To constrain the stratigraphical framework of the slope–mound system and identify and correlate erosional surfaces observed in seismic sections with global palaeoceanographic events, two further sites, located down- and upslope from Challenger mound (sites U1316 and U1318, Fig. 1) were drilled. This study focuses on IODP Site U1318 (51°26.16′N, 11°33.0′W) located in the eastern part of the Porcupine Basin at the upper slope edge of the continental margin of Ireland.

Dinoflagellate cysts and other organic-walled phytoplankton are frequently used as a tool for unravelling biostratigraphical relationships in the Neogene of the North Atlantic realm (Costa & Downie, 1979; Brown & Downie, 1984; Head, Norris & Mudie,1989*a*,*c*; de Verteuil & Norris, 1996) and for the reconstruction of the palaeoenvironment (Louwye, Head & De Schepper, 2004; Piasecki, 2003; Versteegh *et al*. 1996; Warny & Wrenn, 2002). This paper details the depositional history and palaeoenvironment in the eastern Porcupine Seabight through a high-resolution dinoflagellate cyst analysis of the Neogene sediment drift sequence at IODP Site 307 in holes U1318B and 1318C. An assessment of the age of the unconformity on which the Belgica mounds are rooted is given, together with a reconstruction of the palaeoenvironment during early Neogene times. Furthermore, highest and lowest occurrences of dinoflagellate cysts are linked to the palaeomagnetic record and provide new absolute ages for dinoflagellate cyst events in the North Atlantic realm.

2. Palaeoceanographic and geological background

The Porcupine Seabight forms a deep embayment in the Atlantic shelf off the southwestern coast of Ireland and is enclosed by shallow platforms, consisting of Precambrian and Palaeozoic rocks: the Slyne Ridge to the north, the Irish continental shelf to the east and Goban Spur to the south (Fig. 1). Only a relatively small opening towards the deeper North Atlantic Ocean is present to the southeast. The underlying structure of the Porcupine Basin is a Middle to Late Jurassic failed rift of the proto-North Atlantic Ocean (Naylor & Shannon, 1982; Moore & Shannon, 1992). The centre of the basin is filled with 10 km of sediments deposited during the Cenozoic post-rift period (Shannon, 1991). Recent sedimentation is mainly pelagic to hemipelagic, although probably reworked foraminiferal sands can be found on the upper slope of the eastern continental margin. The main sediment supply zone is located on the Irish and Celtic shelves, whereas input from Porcupine Bank seems to be rather limited (Rice *et al*. 1991).

High-resolution seismic profiles through the Belgica mound province perpendicular to the slope reveal that the coral banks are rooted on a continuous but irregular erosional surface (De Mol *et al*. 2002). In the mound area, this erosional surface forms the boundary between seismic units P1 and P3 (Fig. 2) and reflects a deeply incised substratum. The seismic facies of the lowermost unit P1 is characterized by gentle basinward-dipping parallel strata (Van Rooij *et al*. 2003). Within a certain depth interval, however, sigmoidal deposits are observed (De Mol *et al.* 2002), interpreted as upslope-migrating sediment waves within a sediment drift unit

https://doi.org/10.1017/S0016756807004244 Published online by Cambridge University Press

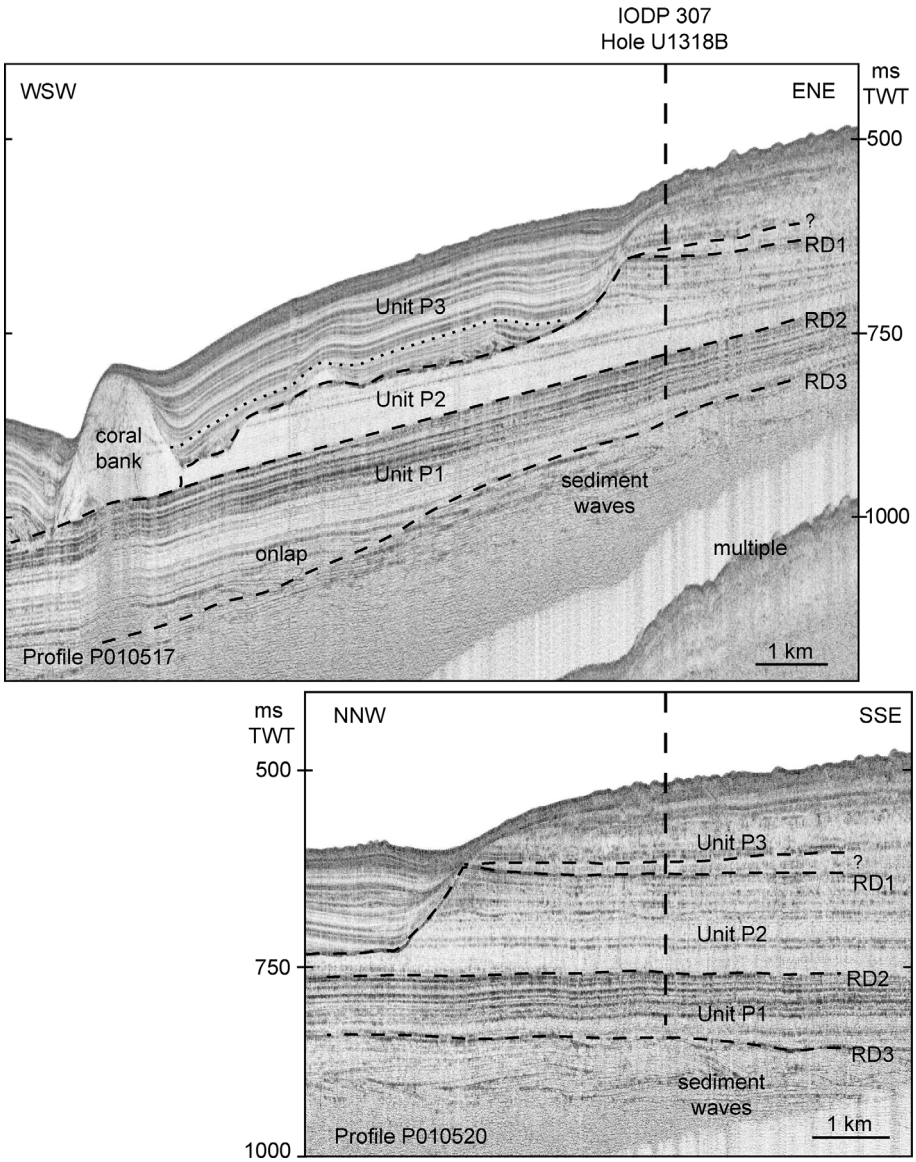

Figure 2. Seismic profiles of the Belgica mound province (for location of the profiles, see Fig. 1), with location of the drill site 1318B, seismic units P1, P2 and P3, and unconformity reflectors RD3, RD2 and RD1 (dashed lines – unconformity reflectors; dotted line – upper limit of drift deposits not observed in U1318B; dashed line with question mark indicates location of a yet unmapped unconformity). Seismograms: Jean-Pierre Henriet, Renard Center for Marine Geology, Ghent University, Belgium.

(Van Rooij *et al.* 2003) (Fig. 2). Unit P3 consists of drift deposits of unspecified late Neogene age (Van Rooij *et al*. 2003). Seismic stratigraphical analyses suggest that the Belgica mounds were already in place before deposition of this unit (Van Rooij *et al.* 2007). The latter authors furthermore state that the mounds were large enough to influence the intensity of the currents and consequently the sedimentary pattern.

The IODP Hole U1318B investigated penetrated seismic units P1, P2 and P3. Due to the upslope position of the site, only the upper part of unit P3 was cored, leaving out the base of the drift unit (Fig. 2). Unit P2 is intercalated between units P1 and P3 and is an acoustically transparent layer characterized by low-amplitude reflectors (De Mol *et al*. 2002; Van Rooij *et al*. 2003). This unit is absent downslope from Hole 1318B. The upper boundary of unit P2 appears erosive and is, according to Van Rooij *et al*. (2003), related to the intra-Neogene margin-wide erosive event RD1. This event eroded units P2 and P1 downslope from Hole 1318B and modelled the palaeotopography before deposition of unit P3 and the onset of mound growth.

Dating of erosional events by De Mol *et al*. (2002), Van Rooij *et al*. (2003) and Van Rooij *et al*. (2007) mostly relied on geometrical arguments, interbasin correlations and correlations with DSDP site 548 on Goban Spur (Fig. 1) (de Graciansky *et al*. 1985; McDonnell & Shannon, 2001; Pearson & Jenkins, 1986; Stoker, van Weering & Svaerdborg, 2001). According to De Mol *et al*. (2002), the erosional surface

https://doi.org/10.1017/S0016756807004244 Published online by Cambridge University Press

on which the Belgica mounds are rooted is of probable Miocene age, while the Unit P3 is of supposed Late Pliocene to Pleistocene age. Van Rooij *et al*. (2003) refine the age model considerably and propose an Early to Middle Miocene age for unit P1, an inferred Middle Miocene–Middle Pliocene age for unit P2 and a Quaternary age for unit P3. The RD2 unconformity between units P1 and P2 at drill site U1318B is caused by an early Middle Miocene erosional event, while the RD1 unconformity between P1 and P3 in the Belgica mound area, and P2 and P3 in the drill site area is related to a Late Pliocene erosional event. Van Rooij *et al*. (2007) propose a Middle Pleistocene age for the onset of the drift sedimentation while the initial settling of coral banks started during Early Pleistocene times.

Van Rooij *et al*. (2003) also presented a reconstruction of the local depositional environment associated with the coral bank settling (Figs 2, 3). Unit P1 was deposited under a relatively calm environment except for a limited zone of the slope where upslope-migrating sediment waves, indicative of strong bottom currents, were deposited. The subsequent erosional event RD2 truncating unit P1 was caused by the introduction of Norwegian Sea Water (NSW) into the North Atlantic Ocean and a wide-spread bottom-current flow under the modern-day oceanographic regime. Following the deposition of unit P2, a margin-wide erosional event during the Late Pliocene significantly eroded unit P2 and P1, creating the irregular and terraced palaeotopography on which coral bank initiation took place. According to the latter authors, this period heralds the influence of the glacial/interglacial variability on the oceanographic regime at the dawn of the Quaternary.

The IODP Hole U1318B investigated was drilled in a water depth of 409 m upslope from the Belgica mound area and recovered 213 m of sediment. A visual description of the sedimentological features is given in Expedition 307 Scientists (2006), who distinguished three lithostratigraphical units (Fig. 3). Unit 1 comprises the interval 0–82.0 m below the seafloor (mbsf) and unit 2 the interval 82.0–86.2 mbsf. Seismic analysis suggests the presence of a yet unmapped unconformity (J.-P. Henriet, pers. comm.) separating lithological units 1 and 2 (Figs 2, 3). A distinct unconformity is observed at 86.2 mbsf and is represented by a 5 to 10 cm thick conglomerate of black pebbles (possibly bivalves) and granules. Unit 3 comprises the sequence downhole from the RD1 moundbase unconformity at 86.2 mbsf to 241.0 mbsf. The sequence is lithologically rather uniform and consists of silty clay, fine-grained sand and clayey silt. The upper 10 cm of unit 3 consists of a distinct bivalve bed unconformably overlain by the conglomerate at the base of unit 2. In general, the carbonate content of unit 3 varies between 27 and 50 wt % (Expedition 307 Scientists, 2006). Within this unit, three subunits can be distinguished. Subunit 3A (86.2–127.4 mbsf) consists

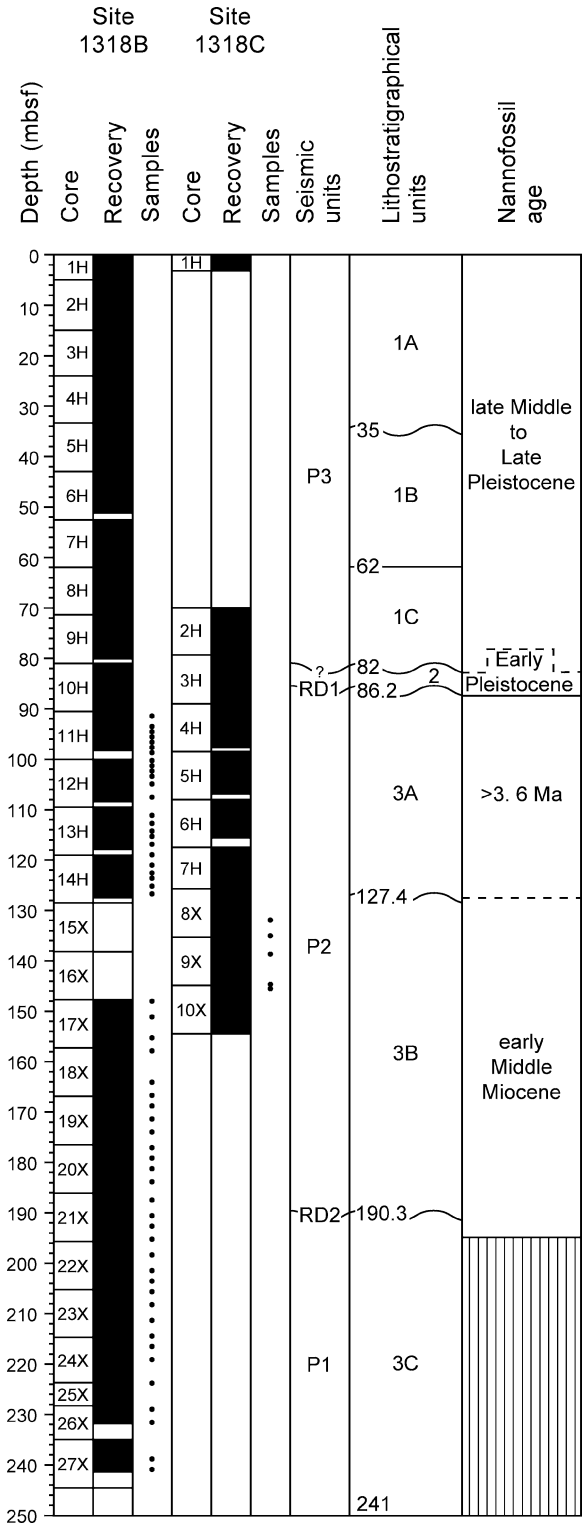

Figure 3. Seismic, lithostratigraphical and biostratigraphical interpretation with calcareous nannofossils of drill Site U1318B. Core recovery (black) and position of studied samples at holes U1318B and U1318C. Wavy lines indicate unconformities, dashed lines indicate uncertain position of boundary.

of silty clays interbedded with well-sorted fine-grained sand and silt with erosive boundaries at their base. Robust bivalves occur sporadically in the upper part of subunit A. Subunit 3B (127.4–190.3 mbsf) consists

https://doi.org/10.1017/S0016756807004244 Published online by Cambridge University Press

of silty clay with a carbonate content varying between 10 and 20 wt %. Bioturbation is abundant. Subunit 3C (190.3–241.0 mbsf) is composed of silty clay to fine-grained sand with a varying carbonate content of approximately 25 to 35 wt %. Bioturbation is abundant and bivalves are rare. Expedition 307 Scientists (2006) correlate the boundary between lithostratigraphical units 3C and 3B with the boundary between seismic units P1 and P2 (Fig. 3).

A biostratigraphical analysis with calcareous nannofossils of core catcher samples from holes 1318A and 1318B was carried out during IODP Expedition 307 and provided a first relative dating of the sediments from Site 1318 (Expedition 307 Scientists, 2006) (Fig. 3). The late Middle Pleistocene to Late Pleistocene *Emiliana huxleyi* Zone (Recent–0.26 Ma) was recognized at a depth of 8.9 mbsf (core 1318A-1H) and 73.6 mbsf (core 1318A-8H). A sample at a depth of 84.6 mbsf (core 1318A-9H) belongs to the small *Gephyrocapsa* Zone and has an Early Pleistocene age. The unconformity at 86.2 mbsf is clearly reflected in the nannofossil record. A sample at 104.3 mbsf (core 1318A-11H), below the unconformity, yields diagnostic species with a highest occurrence at 3.6 Ma, which implies an Early Pliocene or older age. Samples 127.3 mbsf (core 1318B-14H) and 186.0 mbsf (core 1318B-20X) yield characteristic early Middle Miocene species. Nannofossils below 195.5 mbsf are badly preserved and a relative dating could not be proposed.

3. Material and methods

3.a. Palynological analysis

In Hole 1318B, lithostratigraphical unit 3 below the RD1 moundbase unconformity was analysed for dinoflagellate cysts and other marine organic-walled phytoplankton. A total of 60 samples were taken at a regular interval from core 11H (upper depth limit: 90.5 mbsf) to the deepest core 27X (lower depth limit: 241.5 mbsf) (Figs 3, 4). As no sediment was recovered from cores 15X and 16X in Hole 1318B, five samples from the corresponding depth interval in Hole 1318C (cores 8X, 9X and 10X) were analysed (Fig. 3). The first step in the processing consisted in the drying of about 30 cc of sample. About 15 to 25 g of dry sediment were prepared using standard palynological maceration techniques at the Research Unit Palaeontology at Ghent University (Louwye, Head & De Schepper, 2004). The chemical processing involves demineralization with hydrochloric acid (HCl) and hydrofluoric acid (HF). Before demineralization, two *Lycopodium clavatum* tablets (batch no. 483216, X = 18583, s = ±764 per tablet) were added for counting the concentration of dinoflagellate cyst and other marine palynomorphs. The residue was sieved on a 16 μm nylon screen and stained with safranin-O. Glycerine jelly was used as a mounting medium, and the slides were sealed with transparent nail varnish. No oxidation or ultrasound treatments were applied since these techniques could have damaged the dinoflagellate cysts or caused selective loss of species.

A minimum of 300 marine palynomorphs, mainly dinoflagellate cysts, green algae and acritarchs, were counted systematically in each slide, and additionally the terrestrial palynomorphs, mainly bisaccate pollen (Fig. 4). Also, the presence of organic linings of foraminifers was noted. The rest of the slide was then scanned for rare species and well-preserved specimens for microphotography. The latter were not included in the count. The preservation of the dinoflagellate cysts varies between moderate to exceptional, and the assemblage can be considered as diverse and rich. Protoperidiniacean cysts are present throughout the section studied, indicating an unlikely preservational bias through oxidation. Photomicrographs were taken with a Zeiss MRc5 camera mounted on a Zeiss Axioplan2 microscope. The taxonomy of the species recorded (Fig. 4) follows Fensome & Williams (2004). The timescale of Lourens *et al*. (2005) is used throughout this paper. The slides are housed in the collection of the Research Unit Palaeontology of Ghent University, Belgium.

3.b. Palaeomagnetic measurements

Shipboard palaeomagnetic measurements were conducted on cores from holes U1318A, U1318B and U1318C. Remanence measurements and alternating field (AF) demagnetizations were performed using a long-core cryogenic magnetometer (2G Enterprises model 760-R), permanently installed on the R/V *JOIDES Resolution*. This instrument is equipped with a direct-current superconducting quantum interference device (DC-SQUID) and has an inline AF demagnetizer capable of reaching peak fields up to 80 mT. The spatial resolution measured by the width at half-height of the pickup coils response is < 10 cm for all three axes, although they sense a magnetization over a core length up to 30 cm. The magnetic moment noise level of the cryogenic magnetometer is $\sim 10^{-9}$ emu or 10^{-6} A/m for 10 cm^3 rock volume. The practical noise level, however, is affected by the magnetization of the core liner ($\sim 8 \times 10^{-6}$ A/m) and the background magnetization of the measurement tray ($\sim 1 \times 10^{-5}$ A/m). Measurements were undertaken using the standard IODP magnetic coordinate system (+x = vertical upward from the split surface of archive halves, +y = left split surface when looking upcore, and +z = downcore). Alternating-field demagnetization of natural remanent magnetization was conducted up to 20 mT in 5 mT steps on core 307-U1318A-1H. Based on this demagnetization experiment (Fig. 5a, b), the other sections were demagnetized at 10 and 15 mT with a spatial resolution of 5 cm. NRM and magnetization after two-step demagnetization were

https://doi.org/10.1017/S0016756807004244 Published online by Cambridge University Press

(a)

Depth (mbsf)	Slide - sample no. (RUP)	Core	Section no.	Interval from	Interval to	Dinoflagellate cysts	*Achomosphaera andalousiensis andalousiensis*	*Apteodinium australiense*	*Apteodinium spiridoides*	*Apteodinium tectatum*	*Batiacasphaera deheinzelinii*	*Batiacasphaera micropapillata*	*Batiacasphaera minuta*	*Batiacasphaera sp. 1 Edwards (1984)*	*Bitectatodinium? arborichiarum*	*Bitectatodinium? serratum*	*Bitectatodinium tepikiense*	*Bitectatodinium sp. ind.*	*Cannosphaeropsis passio*	*Cerebrocysta poulsenii*	*Cleistosphaeridium placacanthum*	*Cordosphaeridium minimum*	*Cousteaudinium aubryae*	*Cribroperidinium tenuitabulatum*	*Dapsilidinium pseudocolligerum*	*Dinocyst sp. 7 Manum et al. 1989*	*Dinopterygium cladoides*	*Distatodinium paradoxum*	*Echinidinium euaxum*	*Echinidinium sp. A*	*Echinidinium sp. B*	*Echinidinium sp. C*	*Echinidinium sp. ind.*	*Edwardsiella sexispinosum*	*Filisphaera filifera filifera*	*Geonettia? sp. ind.*	*Habibacysta tectata*	*Hystrichokolpoma rigaudiae rigaudiae*	*Hystrichosphaeropsis obscura*	*Hystrichostrogylon membraniphorum*	*Impagidinium aculeatum*	*Impagidinium pallidum*	*Impagidinium paradoxum paradoxum*
91.7	1	11H	1	123	125		2				+	2	2	+					5	+					1	+										11					+
93.7	2	11H	3	23	25		1				1		7	+	1				7	1					2	1	+									10	+	+			+
94.7	3	11H	3	123	125		+				2		5	+	1	+			11	+		1			4	+	2									19		+			
95.2	4	11H	4	23	25		2				+		6	+	5				5	+					4	+	1									39	+	2		+	+
96.2	5	11H	4	123	125		3			+	1		3			1			11	+	1					1						+				34		+		+	+
96.8	6	11H	5	23	25		1				4		12	+					9			+			3	5								+		19		1			+
97.8	7	11H	6	23	25		9				1		14	1		+	+		+	+		1			11					1				+		11		3		2	+
100.2	8	12H	1	23	25		2	+			4		+	+	+				2	+	1	1			3	+										17		1			
101.2	9	12H	1	123	125		1				6	1	+	+		+				+	+				3											17		2			+
101.7	10	12H	2	23	25		2				+	1	3	+						+		1			5											15	+	+	+	+	1
103.3	11	12H	3	23	25		1				+		3	+			+			2	+	+			9											4	1	+	+		+
104.8	12	12H	4	23	25								1	+				1				2			3	+										13	1	1	1		
107.8	13	12H	6	23	25		2					+		+						10	1	3			9											27	1	2	2	2	+
111.2	14	13H	2	23	25		+				1		3				+			4		1	+		4	2										16	2	+		1	1
112.7	15	13H	3	23	25						+		+	1			+			+		+			2	1										106	2	+	+		+
114.2	16	13H	4	23	25						+		2							3					6					1						97	+	+			1
115.7	17	13H	5	23	25		1				1	1	2	+		1	1			3		1			7											37		1			1
117.3	18	13H	6	23	25		1					1	1	1						+		1			5											45					1
119.2	19	14H	1	23	25						2	1	6	+						+	1				1				+	+		+				85	1	+		+	+
120.7	20	14H	2	23	25							2	1	+			2			1	2	+			2				+							68	4	+		+	1
122.3	21	14H	3	23	25					+	1	3	1	1			+				7	2	+		1						+					10	14	+		1	
123.8	22	14H	4	23	25							4	8	+						2	1				7					1						41		+		+	+
125.3	23	14H	5	23	25		+			+		1	1	+			+								2			+		+						35	1	+		+	14
125.6	24	14H	6	23	25		1					1	+	+						8	1	1			4			+			+						17	+	1			1
132.0	117	8X	5	36	38		2						4	3									1		8	6						4			2	30	1				
135.0	118	8X	7	35	37		2						3	3			1			+	1				6	5	+								1	10	1	1		2	
138.6	120	9X	3	30	32					1			13								15			15	7	5									3	1	2		1	
144.6	122	9X	7	29	31				+	+	3		15	1							5		+	3	9	+	2					+	3	+			3	+			
145.9	123	10X	1	102	104					1	11		7	+			1			+					1	2	2						2				+			1	
147.9	25	17X	1	23	25					+	5	2	19							+	9	1			1		3			+	+					1					+
150.9	27	17X	3	21	23					13	8		5				+				6	+	+		7		+			1	+	1				1	+			1	
155.6	29	17X	6	33	35					4	4	14	27	+						+		2			11		6			4	3					2	1				
157.9	31	18X	1	33	35					5	2	8	9	+								2	+		2		3	+		+						5	2			+	2
164.2	33	18X	5	33	35				+	3	1	1	3				+				9	1	+		8		10		1							3	+			1	
166.4	34	18X	6	108	110					+	4		5	+							6		+		10		6						1			3	1				
169.0	36	19X	2	33	35				+	2		5	9				+				5		+		+		3		+	+	4					1	+			1	
171.5	38	19X	4	33	35				+	+	2	11	13	1							10	2	+		8		12		+	+						+					+
174.0	40	19X	6	33	35					1	5	12	18								5	3	+		1	+	4		1	+						3	+			+	
176.5	42	19X	8	33	35					1	1	4	2	1							5	1	7		1		3									1	+				
178.9	44	20X	2	32	34					13	1	4	9	1						1	10	1	7	+	5		2		1	+						2	1			+	
181.4	46	20X	4	33	35				1	2		3	12	+						1	13	1	10	+	5		1				+	+	2			1	+			+	
183.9	48	20X	6	33	35					+		3	12								23	4	5	1	3	+	+									+	2			1	1
187.3	50	21X	1	28	30					+	1	2	2	+						+	18		4	2	2	1	1	+	+	1	1						+			1	
190.3	52	21X	3	29	31					2		1	3	1						1	14		21	3	3		1			+		4				+	+			
192.8	54	21X	5	28	30					2		7	12	1						3	25	1	8	12	16	+										1			2	1
195.3	56	21X	7	33	35					4	1	4	6							1	17		5		4		2	+								1	+			1	
198.3	58	22X	2	33	35					7	1	3	3							+	41	1	13		3		1	3				+				+				1	
200.8	60	22X	4	33	35					16		2	7							+	25		20	+	+			5				1				1					+
203.2	62	22X	6	31	33					8	1	1	7							+	35		18			+		2				+				2	+				
205.7	64	22X	8	28	30					9		4	3								50	1	11	10	4		1	1												+	
208.1	66	23X	2	31	33					9		5	5							3	24	1	3	1	7	+	3					+				+	+			+	
211.1	68	23X	4	32	34					12		2	14								56		16	5	2	1	2	2								2	+				
214.1	70	23X	6	32	34					5		1	2							1	51	1	28			1	5	1								+	1			2	
216.4	72	24X	1	32	34					6		2					1			1	46		14	3	8			5								+					
219.4	74	24X	3	32	34					1			4								65		47	4	1		3	+				1					1			+	
223.8	76	24X	6	32	34					+		1	4								52	1	38	6	1		1	1				1				+					
228.7	79	25X	3	77	79					1		1								1	46		##	2	2			1										+			
231.3	81	26X	2	39	41					1		2	1							1	20		26		4		4	1				1					+			+	
238.6	83	27X	2	13	15				+	2		1	1							+	30		56		9	+		7				+									
241.3	86	27X	5	10	12					8		2	4								28		50		5											1					

Figure 4. (a, b, c) Distribution of dinoflagellate cysts and other organic-walled palynomorphs in holes 1318B and 1318C. For location of samples see Figure 3. (Continued)

https://doi.org/10.1017/S0016756807004244 Published online by Cambridge University Press

(b)

Depth (mbsf)	Slide - sample no. (RUP)	Core	Section no.	Interval from	Interval to	*Impagidinium patulum*	*Impagidinium striadatum*	*Impagidinium sp. ind.*	*Invertocysta lacrymosa*	*Invertocysta tabulata*	*Labyrinthodinium truncatum modicum*	*Labyrinthodinium truncatum truncatum*	*Lejeunecysta hatterasensis*	*Lejeunecysta marieae*	*Lejeunecysta sp. A*	*Lejeunecysta spp. ind.*	*Linguladinium machaerophorum machaerophorum*	*Linguladinium multivirgatum*	*Melitasphaeridium choanophorum*	*Nematosphaeraopsis labyrinthus*	*Operculodinium? borgerholtense*	*Operculodinium centrocarpum centrocarpum*	*Operculodinium? eirikianum*	*Operculodinium israelianum*	*Operculodinium longispinigerum*	*Operculodinium piaseckii*	*Operculodinium sp. A*	*Operculodinium spp. ind.*	*Organic membrane of calcareous cyst*	*Palaeocystodinium golzowense*	*Pentadinium laticinctum laticinctum*	*Polykrikos sp. ind.*	*Polysphaeridium zoharyi*	*Pyxidiella? simplex*	*Pyxidinopsis tuberculata*	*Pyxidinopsis sp. ind.*	*Reticulatosphaera actinocoronata*	*Round brown cysts*	*Selenopemphix brevispinosa*	*Selenopemphix dionaeacysta*	*Selenopemphix nephroides*	*Selenopemphix quanta*	*Selenopemphix sp. A*
91.7	1	11H	1	123	125							5			+	4		1	3		2	+	3	+	+	2			1						1	1					
93.7	2	11H	3	23	25	+				+		1			+	15		3	6		6	+	9	1	+	1	1							+	3						
94.7	3	11H	3	123	125							1			1	5		4	7		7		4					+		+				+		1					
95.2	4	11H	4	23	25	1						3		+		11		+	5		1	1	3			2		+	+					1		3	+				
96.2	5	11H	4	123	125	+			2			4				5		4	4		12	1	4	+	1			1	+	+		+	2		5						
96.8	6	11H	5	23	25	+			+			+				4		4	11		7	1				3			+	1		+	+		4	1					
97.8	7	11H	6	23	25		+					4		+		4		1	7		8	17	1		1	3		+	1	+				+		3	3	+	+			
100.2	8	12H	1	23	25		+					+				5		3	1		7	6	8					+	1	+				1		4	2					
101.2	9	12H	1	123	125				+			4	+			6		2	2	+	36	2	2		+	2		+		+				1			2					
101.7	10	12H	2	23	25				+			3			+	3		4	1	+	7		8			+	+	3		+				+		1	+		+			
103.3	11	12H	3	23	25	+						8				5		1	3	3	7	+	2		+	+		+		1				+	1	1			1			
104.8	12	12H	4	23	25		+	+				3			2	4			8	+	12		3	+	2	1		1	+	+					2	12			1			
107.8	13	12H	6	23	25				2			3			1	14		2	7	+	10							+						+	2	1						
111.2	14	13H	2	23	25	+						1			+	16		+	2		5		5				1	+	+	2		1		+	+	6						
112.7	15	13H	3	23	25	+						4			+	11			5	+	12	2				+		+	+				+	+	2	+					
114.2	16	13H	4	23	25	+				+		2			+	5		+	9		16	+					3	2		+			+	3	6			1	+		
115.7	17	13H	5	23	25				+		+	3				33			2	+	4		2		+	1	1		+	1				2		1					
117.3	18	13H	6	23	25	+					+	2				13		+	8	+	6	1			+			+				+	+	2							
119.2	19	14H	1	23	25						1	+		+		5		+	10	1	3		1		+			+	+	+			1		7			2			
120.7	20	14H	2	23	25						2	10				5		1	6	+	14							+	+	+		+	+		+						
122.3	21	14H	3	23	25	+		+				1				15		2	3	+	8	1						+	1	+			+		+	+		2			
123.8	22	14H	4	23	25	3			+		2	1				9		1	6		7							+	2	+			1		5	4		+	+		
125.3	23	14H	5	23	25	+				+		19		1		4		1	7		10	1							+	2	+		2	2	1	5		1			
125.6	24	14H	6	23	25	+			+	1		4				2		+	6	+	1	6					+	1	+				2		8	1		+			
132.0	117	8X	5	36	38			6		+		10			3	9		1	5		3				+				23				2		+	1	+				
135.0	118	8X	7	35	37			2				9			1	9		6	4		11	+		1	1			+	23				1		+	+					
138.6	120	9X	3	30	32		1	+		1		6			+	20		+	+		8							+	20				2		5	2	+				
144.6	122	9X	7	29	31		+	1	+	+		6				8		5	3		16				+			+				1		3		+	1				
145.9	123	10X	1	102	104			2	7	5	1	2		+	+	2	13		1	9	1	11			1				+	1					3	9	+		+		
147.9	25	17X	1	23	25						+	2		1	+	1	30		1	3	3	6			+		+			1			+	1		7	3	1		3	1	
150.9	27	17X	3	21	23							2				+	11		4	+		10	+		1			2	+				+	+		6	1	1		1	1	
155.6	29	17X	6	33	35							1		1	+	4	14			2		3		2			+	+		2			+			2	3	5		1	2	
157.9	31	18X	1	33	35							1				+	16			+	3	14			+		+		+	5			8		+		5	1	+		1		
164.2	33	18X	5	33	35	+						1		2		1	17		1	2	1	4				1			1	2			+		+		5	8	+		+		
166.4	34	18X	6	108	110							6		+			26		4	2		6			2								+		+		1	6					
169.0	36	19X	2	33	35						+	2			1	3	11		+	+		5				+			1	1			1		+		+	6	+		+	1	+
171.5	38	19X	4	33	35							6		1	+	3	33			3		2				2			1	1					+		3	13	1		+	3	+
174.0	40	19X	6	33	35							2			2	1	23		2	7	+	8							2	1			+	1	+		1	9	1		1	+	+
176.5	42	19X	8	33	35					1		2			+	1	12		1	2		6			3					1	+		+		1		3	+			+		+
178.9	44	20X	2	32	34					+	2	4				4	35		1	1				2				+		+			2		7		6	5	1		2		
181.4	46	20X	4	33	35						+	+		+	+	1	22		2	1	1			3				+	+	3			2		1	1	5	1	1		1	+	
183.9	48	20X	6	33	35					+	2	+			+	+	19		1	2	2	7					+		+	2	+		5	1	2		3	6	+				
187.3	50	21X	1	28	30	+				+	5	2			+	2	14		7	6	3	5			+				+	2	3		1		+		2	2	+		4		+
190.3	52	21X	3	29	31							+			+	3	12		+	1		6							2	1			2	1			1	2				+	
192.8	54	21X	5	28	30	+					5	2			1	3	13		2	9		3								2			9				1	3	1		2		+
195.3	56	21X	7	33	35						+	1			+		16		1	2	1	3							+	2	+		11				+						
198.3	58	22X	2	33	35						1					+	13		2			6				+			+		+		6		+		8				+		
200.8	60	22X	4	33	35							1			1		5		+			1			1				1	+			6		1		4	2			1		+
203.2	62	22X	6	31	33	+								1	+		4		1	2		16		1		1			2	2			12				5	5			1		
205.7	64	22X	8	28	30										+	1	8		3	+		12							+	1			2		+		4						+
208.1	66	23X	2	31	33	2					2				+	4	3		2	1		4		1					+	5	+		6		+			+	+		+		+
211.1	68	23X	4	32	34							+				1	2		3	1	2	6		1						1	+		5				4	+					
214.1	70	23X	6	32	34	+					3			1	+	1	9		1	3										1	+		2		+		3	3			+	+	
216.4	72	24X	1	32	34	+					1	1					4		2		+	2		1		+							2				3						
219.4	74	24X	3	32	34										+		5		2	2		9		+						3			7				3	1					
223.8	76	24X	6	32	34												8			+		3		1					3				1				3	1					
228.7	79	25X	3	77	79	+											4		1		1	1		2		1			1				1				1						
231.3	81	26X	2	39	41	2					2				+	1	12	3		6		10								+	+		1		2		3	+					
238.6	83	27X	2	13	15										1		6		1	+		14		1						8			1		+		6	8			1		
241.3	86	27X	5	10	12												1		+			7							+		1		5	+	+		+				+		

Figure 4. (Continue)

https://doi.org/10.1017/S0016756807004244 Published online by Cambridge University Press

(c)

Depth (mbsf)	Slide - sample no. (RUP)	Core	Section no.	Interval from	Interval to	*Selenopemphix spp. ind.*	*Spiniferites/Achomosphaera complex*	*Sumatradinium druggii*	*Sumatradinium hamulatum*	*Sumatradinium soucouyantiae*	*Tectatodinium pellitum*	*Trinovantedinium ferugnomatum*	*Trinovantedinium harpagonium*	*Trinovantedinium glorianum*	*Trinovantedinium? xylochoporum*	*Trinovantedinium sp. A*	*Trinovantedinium sp. ind.*	*Tuberculodinium vancampoae*	*Unipontedinium aquaeductum*	**Total *in situ* dinoflagellate cysts**	***Acritarchs***	Acritarch sp. 1 Head et al. 1989	*Cyclopsiella elliptica/granosa*	*Cyclopsiella? trematophora*	*Cyclopsiella sp. A*	*Cyclopsiella sp. ind.*	*Cymatiosphaera bafffinensis*	*Cymatiosphaera sp. ind.*	*Leiosphaeridia sp. A*	*Nannobarbophora gedlii*	*Palaeostomocystis globosa*	*Paralecaniella indentata*	*Quadrina condita*	*Small spiny acritarch*	**Green algae**	Tasmanites	**Total organic-walled palynomorphs**	**Other marine microfossils**	Foraminiferal test lining	**Total reworked dinoflagellate cysts (undiffer.)**	**Terrestrial palynomorphs**	Non-bisaccate pollen and spores	Bisaccate pollen
91.7	1	11H	1	123	125		241													287										+						289	5	2			2
93.7	2	11H	3	23	25		209											+	1	287								1		+		+				288		1			3
94.7	3	11H	3	123	125		202			+	+							+		278										+						278		1			2
95.2	4	11H	4	23	25		298			1	+							1		395			1		+					+						396		2			4
96.2	5	11H	4	123	125		208				+								+	308					+					1						309	+	1			1
96.8	6	11H	5	23	25		190				+									280					+					2			+		+	282	2	1			
97.8	7	11H	6	23	25		226	+		3								+	+	336										1	1		7			346	8				3
100.2	8	12H	1	23	25		247		+	+								+		319										2	+					321	11	1			1
101.2	9	12H	1	123	125		230			3	1							1	+	324			1	+						9						334	5	2			1
101.7	10	12H	2	23	25		202	3	+	+	1							1	2	272										4			3			279	1	1			
103.3	11	12H	3	23	25		236	+		+	+							+	+	289										7						296	1	1			
104.8	12	12H	4	23	25		216	+			+						+	+	1	291								+		9					+	300	4	3			1
107.8	13	12H	6	23	25		200		+	1								1	1	306										7	+					313					1
111.2	14	13H	2	23	25		250		2	1	5				+			+	3	336										4			7			347					3
112.7	15	13H	3	23	25		195		1	+	+				+			1		345							+			6			3		+	354	+	1			
114.2	16	13H	4	23	25		152	2	+	2						+	+	1	9	327							1		+	9						337	1	1			1
115.7	17	13H	5	23	25		190	+			1							+	2	300							2			+			3			305	2				3
117.3	18	13H	6	23	25	+	233	2		1	1							+	1	326										1	+		3			330	1	1			7
119.2	19	14H	1	23	25	1	207	+		2	1						+	+	6	348										3	3		1			355	6	1			7
120.7	20	14H	2	23	25		204				+	+						+	+	325										+	+			1		326	1				1
122.3	21	14H	3	23	25		206			1	+							1	3	285		1								+	1		1			288	1	1			3
123.8	22	14H	4	23	25	+	281		1	+					+				2	389				+			+			+			2			391	3				4
125.3	23	14H	5	23	25	1	240		1	1	1			+	+				2	357										4			1		+	362	12	1			3
125.6	24	14H	6	23	25		306	+	2	1	1							+	12	390																390	2				3
132.0	117	8X	5	36	38	2	298			6	+						1	+	8	439			22													461	3	2		3	16
135.0	118	8X	7	35	37		299		1	2	1							1		409			+													409	1				4
138.6	120	9X	3	30	32		312	2	+	2	+					1		5	1	452	1	2					1						4			460	2	4			22
144.6	122	9X	7	29	31		301	2	3	1	+					+	1	+	+	396													2	+		398	1				27
145.9	123	10X	1	102	104		301	1	1	2	+					+			3	404		1					3						1	+		409	11			1	7
147.9	25	17X	1	23	25		255	1	1	+					+			1	+	363		6	3				4									376	9				14
150.9	27	17X	3	21	23	7	273	1	+	4	+		5					+	+	373		+					1									374	7				10
155.6	29	17X	6	33	35	5	234	2	+	4	2					1		+		368		2					2						1			373	12	1			54
157.9	31	18X	1	33	35	1	306	1	1	4	1							+		408													3			411	4				16
164.2	33	18X	5	33	35		325	2	+	3	2				+	1		+		420		1	1				+									422	1				10
166.4	34	18X	6	108	110		262		+	1						1	1			354			1		1		2									358	4				18
169.0	36	19X	2	33	35	7	249	1	+	1	+					1		+		321		5					2				1		2	+		331	4	1			12
171.5	38	19X	4	33	35	3	286	1		2				1		+	1	1		426							3				2			+		431	5				28
174.0	40	19X	6	33	35	7	262	2		5	+			1		+		4		395		16					1				1			1		414	1				20
176.5	42	19X	8	33	35	1	290	+		+	+							+		351		2					+				9		1	+		363	2	1			3
178.9	44	20X	2	32	34	3	301	+		2						1		1		438		2											1	+		441	3				29
181.4	46	20X	4	33	35	9	309	1		2	+				+	+		2		420		1	+								+		1			422	4	13			13
183.9	48	20X	6	33	35	7	302	+	+	+	+							1		417		2	+											+		419	11	6			22
187.3	50	21X	1	28	30	7	345	+			1						+	1		448		1	+													449	4	1			9
190.3	52	21X	3	29	31	1	293	2							1	+		1		383		19	1				2						2	+		407	5	4			21
192.8	54	21X	5	28	30	9	294	1		2	+									453							2						1		1	457	9	4			62
195.3	56	21X	7	33	35	6	302			3	3									397							+						3			400	3	1			31
198.3	58	22X	2	33	35	2	311	+		1	1				+			+		428				+									3		+	431	6	2			17
200.8	60	22X	4	33	35	1	305	+		3	+									410						+	1				+				+	411	11	1			46
203.2	62	22X	6	31	33	7	317	3	+	5					+			+		459		3					1				1		+		1	465	11				61
205.7	64	22X	8	28	30	1	304	4	+	7				1						442		+					1				1		+		+	445	7	1			74
208.1	66	23X	2	31	33	3	313	4		+	+			1				+		412		+									+		+		+	412	7	1			19
211.1	68	23X	4	32	34	9	305	1		1	+							+		456		2					+						+			458	6	1			35
214.1	70	23X	6	32	34	+	303	1	+	12	+	1								443		+					+				+	1	+			444	3	1			23
216.4	72	24X	1	32	34	+	306	1	+	1								+		410							1						+			411	2	2			12
219.4	74	24X	3	32	34	+	318		+	1							+	+		478		3										1	+			482	1				21
223.8	76	24X	6	32	34	2	310	+		2	+							+		440		+									+		+		+	440	1	2			11
228.7	79	25X	3	77	79	2	303			1	2				+			1		513		1		+	1						1	+		+			516	7	3			4
231.3	81	26X	2	39	41	3	300	+		4		+						+		410							+									410	1	2			8
238.6	83	27X	2	13	15		303	2		1								+		459		+									+		4	1		464	12	3			28
241.3	86	27X	5	10	12		301	+		2	+									415					1		+							+		416	5	3			14

Figure 4. (Continue)

https://doi.org/10.1017/S0016756807004244 Published online by Cambridge University Press

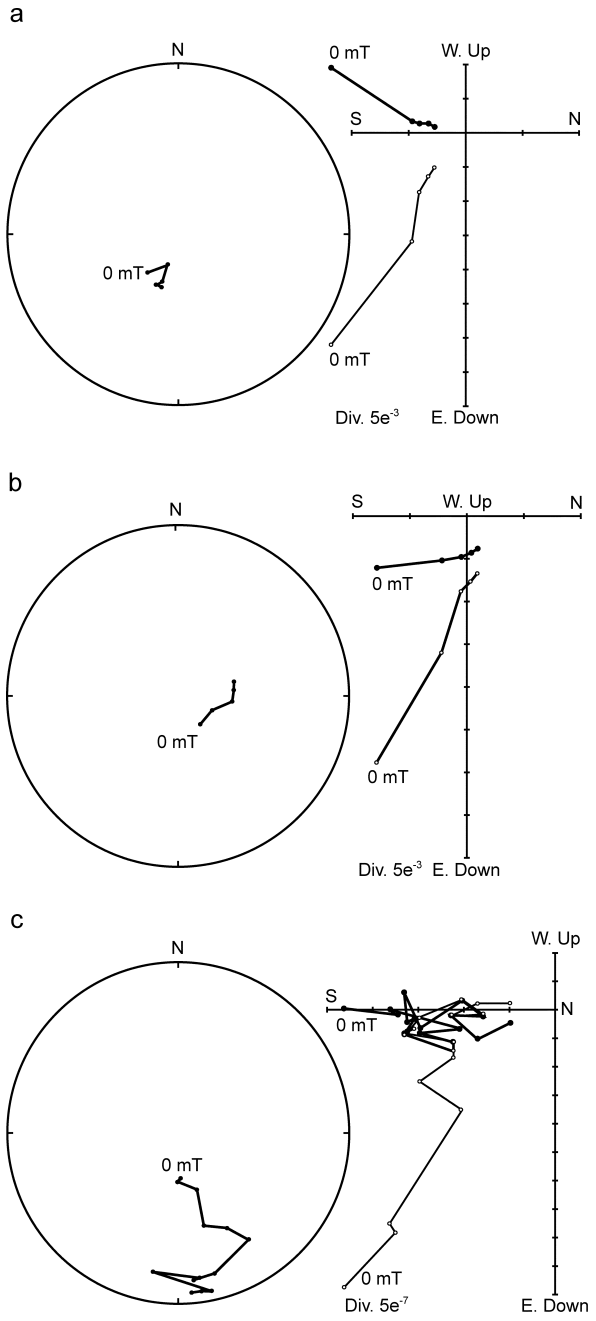

Figure 5. (a) Stepwise AF demagnetization (5, 10, 15, and 20 mT) of Section 307-U1318A-1H1 at 0.25 mbsf. (b) Stepwise AF demagnetization (5, 10, 15, and 20 mT) of Section 307-U1318A-1H3 at 3.15 mbsf. (c) Stepwise AF demagnetization (0, 2.5, 5, 7.5, 10, 12.5, 15, 17.5, 20, 22.5, 25, 30, 35, 40, 45, and 50 mT) of Section 307-U1316A-2H5 at 164.5 mbsf. Left panels represent orthogonal projections of endpoints of the magnetization vector. Open circles – projections on vertical plane; solid circles – projections on horizontal plane. Right panels represent equal area projection of the magnetization vector during demagnetization.

measured on archive halves. Discrete samples were taken on the working halves of cores in Hole U1318B.

Shore-based measurements were carried out with the cryogenic magnetometer (2G Enterprises model 760-R) installed at the geophysical centre of Dourbes (KMI, Belgium) and equipped with direct-current superconducting quantum interference device (DC-SQUID) magnetic sensors. An inline AF demagnetizer has the capability to reach peak fields up to 100 mT. The SQUID-sensors can detect magnetizations up to 10^{-12} A/m. The more precise detection limit, compared to the same instrument installed aboard the *JOIDES Resolution*, can be explained by lower interference of magnetic and electrical noise. The measurements on the discrete samples confirmed the isolation of the characteristic remanent magnetization for the uppermost sections at 10–15 mT. Obtaining stable remanent magnetizations in the lowermost sections was difficult (Fig. 5c). However, characteristic remanent magnetizations could be calculated by the standard three-dimensional least-squares fit to palaeomagnetic vector data via principal component analysis (PCA) on AF-demagnetization steps 7.5 mT, 10 mT and 12.5 mT, respectively (Kirschvink, 1980). Visualization and analysis of the palaeomagnetic data were performed in the windows-based 'palaeomagnetic analysis program', developed by Zhang & Ogg (2003).

4. Discussion of the organic-walled phytoplankton assemblage

A total of 89 *in situ* dinoflagellate cyst species, 13 acritarch species and one green alga were recorded (Fig. 4). Every sample is dominated by the *Spiniferites*/*Achomosphaera* spp. group. Neogene species of the genus *Spiniferites* are usually thin-walled and easily recognized. However, they have a limited biostratigraphical potential, which is the reason for the incorporation in this large amalgam of species. The notable exception, *Achomosphaera andalousiensis andalousiensis*, has a lowest occurrence (LO) in the upper part of the Serravallian (Gradstein, Ogg & Smith, 2005), and was therefore not included in the group. Thick-walled representatives of *Spiniferites* spp. are recorded in every sample, and it is probable that a small number of them are to be considered as reworked from the Cretaceous. Since no distinction was made between Neogene and pre-Neogene *Spiniferites* and *Achomosphaera*, the size of this allochthonous component of the assemblage remains unknown. Reworking of other pre-Neogene species is relatively unimportant and never exceeds more than 3 % of the assemblage (core 1318B-20X). Although not detailed in Figure 4, reworking of Cretaceous species is more frequent than of Palaeogene species.

Batiacasphaera micropapillata, *Batiacasphaerta minuta*, *Dapsilidinium pseudocolligerum*, *Lingulodinium machaerophorum machaerophorum*, *Nematosphaeropsis labyrinthus* and *Operculodinium centrocarpum centrocarpum* are abundant species in almost every sample. *Cousteaudinium aubryae*

https://doi.org/10.1017/S0016756807004244 Published online by Cambridge University Press

and *Cleistosphaeridium placacanthum* are present abundantly in the lower part of the section studied, respectively, in cores 1318B-17X to 27X, and in cores 1318B-18X to 27X. In the latter cores, *Polysphaeridium zoharyi* is present continuously. *Unipontedinium aquaeductum* was recorded in the assemblage from core 1318B-17X through 11H, that is, the upper part of the core. *Habibacysta tectata* is present in large numbers in every sample of cores 1318C-9X through 1318B-11H. The remainder of the assemblage is present in considerably lower numbers. The heterogeneous group 'Round Brown Cysts' mostly comprises thin-walled dark brown cysts with probable *Brigantedinium* affinities. The preservation of these heterotrophic cysts is moderate to poor and hinders a specific determination. A selection of dinoflagellate cysts species in open nomenclature is given in Figure 6.

5. Review of selected Lower and Middle Miocene dinoflagellate cyst studies in the North Atlantic Realm

A detailed and comprehensive account of global Miocene dinoflagellate cyst studies is given in Head, Norris & Mudie (1989*c*). These authors discuss in great detail the biostratigraphical studies with dinoflagellate cysts from mostly DSDP and ODP sites in the North Atlantic realm and contiguous areas: Norwegian–Greenland Sea, DSDP Leg 38 (Manum, 1976), Rockall Plateau, DSDP Leg 48 (Costa & Downie, 1979), Denmark (Piasecki, 1980), Goban Spur, DSDP Leg 80 (Brown & Downie, 1984), Rockall Plateau, DSDP Leg 81 (Edwards, 1984) and Vøring Plateau ODP Leg 104 (Manum *et al*. 1989). According to Head, Norris & Mudie (1989*c*), sample resolution and dinoflagellate cyst diversity and richness in the latter studies is mostly high, while the availability and quality of the independent biostratigraphical control is highly variable. Traditional biostratigraphical control is usually provided by calcareous nannoplankton and foraminifers, and only a few sites have stratigraphical control through magnetostratigraphy or radiometric dating. The dinoflagellate cyst biozonations from these sites have not only been refined or redefined during the last decades, the chronostratigraphical position of the dinoflagellate cyst events has altered many times since their publication. In light of the recent advancements in Lower and Middle Miocene biostratigraphy and the publication of a new Neogene timescale (Lourens *et al*. 2005), it is necessary to review certain aspects (ranges of key species, ages of boundaries) of these biozonations. Furthermore, recent studies made clear that many of the discrepancies in the stratigraphical ranges of some species between sites are related to differing palaeoenvironmental conditions, such as sea-surface temperature, upwelling and palaeodepth of the depositional area. A brief re-evaluation of some Lower and Middle Miocene key species with stratigraphical or palaeoecological significance from the above mentioned studies, and present in this study, is therefore given (Fig. 7).

5.a. Baffin Bay–Labrador Sea

Head, Norris & Mudie (1989*a*,*b*,*c*) reported on Miocene and Lower Pliocene high-resolution dinoflagellate cyst studies from Baffin Bay (Upper Miocene to lowermost Pliocene: Hole 645E, Leg 105) and from the Labrador Sea (Lower Miocene to lower Upper Miocene: Site 646, Leg 105). Approximately 100 dinoflagellate cyst taxa were recovered from the Lower to Middle or lower Upper Miocene in Hole 645E in Baffin Bay. Five dinoflagellate cyst biozones are defined (BB1 to BB5), and ages mainly rely on dinoflagellate cyst datums, and where available, on biostratigraphy with other microfossils and magnetostratigraphy. Biozones BB3 and BB4 are of Middle Miocene age. The LO of *Labyrinthodinium truncatum* defines the lower boundary of zone BB3, and is considered as an important datum. Other species with a LO within this zone are *Invertocysta tabulata* and *Habibacysta tectata*. The base of zone BB4 is defined by the LO of *Unipontedinium aquaeductum*. The upper boundary of zone BB4 is defined by the LO of the acritarch *Leiosphaeridia* sp., and tentatively placed in the late Middle Miocene or early Late Miocene. Unfortunately, the age of this zone is poorly constrained by other microfossil groups.

5.b. Salisbury Embayment, USA

De Verteuil (1996, 1997) and de Verteuil & Norris (1996) published their results of the biostratigraphical analysis with dinoflagellate cysts of the continental slope and rise off New Jersey (ODP Leg 150), the Cape May and Atlantic City boreholes (New Jersey Coastal Plain, USA), and the Miocene in the Salisbury Embayment (Atlantic margin, USA). Their zonation covers the uppermost Oligocene to the uppermost Miocene and holds ten biozones with an average zonal duration of 1.8 Ma (Fig. 7). The biostratigraphical study is mostly based on classic onshore Miocene sections but the data was integrated with planktonic foraminiferal and calcareous nannofossil biostratigraphical data from ODP Leg 150. The zonation proved readily applicable to Miocene successions from other mid-latitude sites such as the North Sea Basin (Louwye, 2002, 2005; Louwye, De Coninck & Verniers, 2000).

The *Cousteaudinium aubryae* Interval Zone (DN3: middle Lower Miocene to upper Lower Miocene) is a 'gap' zone defined as the interval from the highest occurrence (HO) of *Exochosphaeridium insigne* to the LO of *Labyrinthodinium truncatum*. The assemblage is characterized by high numbers of the eponymous species *Apteodinium spiridoides* and *Cleistosphaeridium placacanthum*. The *Distatodinium paradoxum* Interval

https://doi.org/10.1017/S0016756807004244 Published online by Cambridge University Press

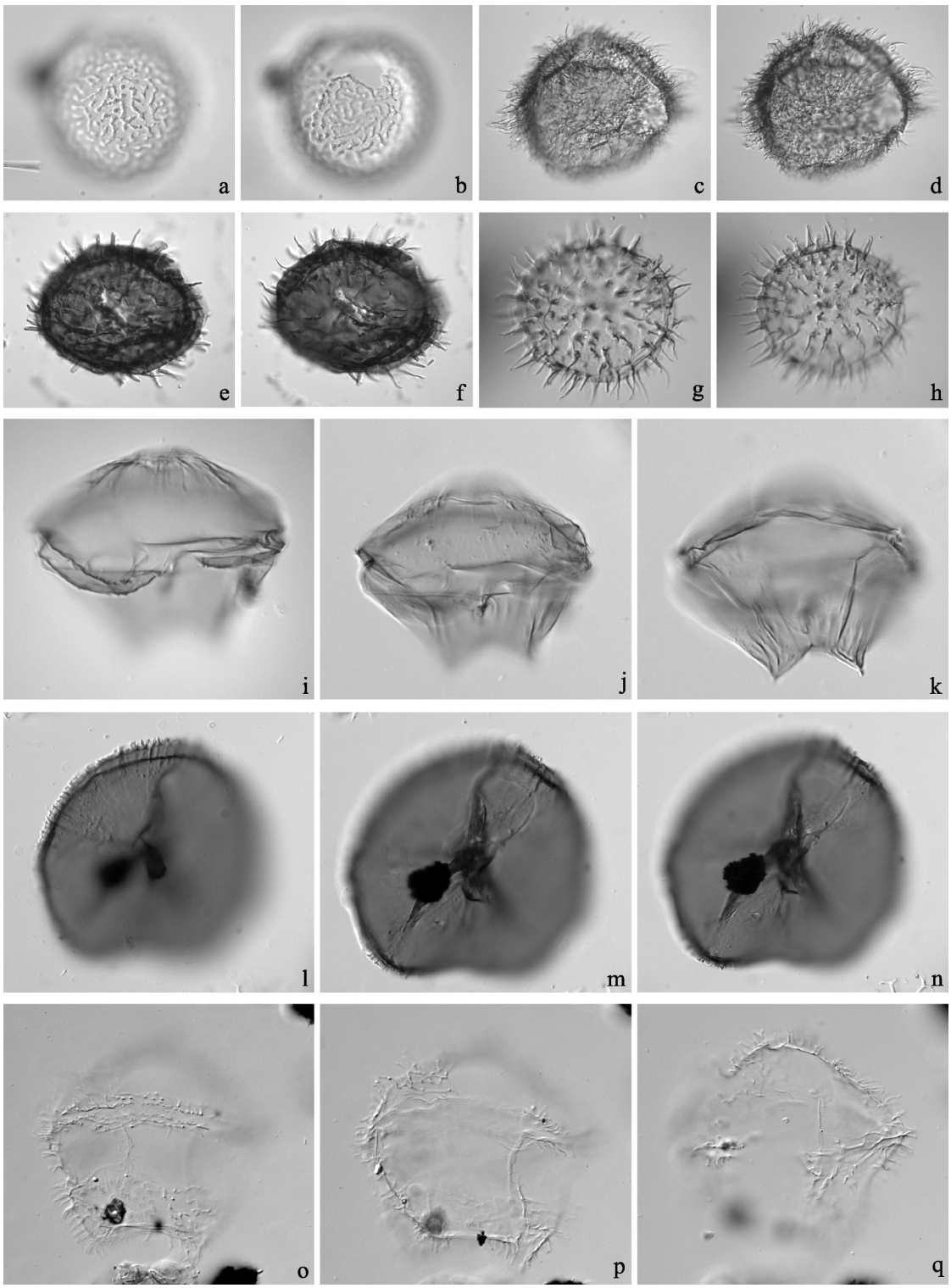

Figure 6. Photomicrographs of selected dinoflagellate cysts from Hole U1318B. All photomicrographs taken in bright field. Various magnifications. (a, b) *Batiacasphaera* sp. 1 Edwards 1984. High focus on ornamentation (a) and low focus on archaeopyle. Maximum width central body 44 μm; wall thickness 2 μm. (c, d) *Echinidinium* sp. A. High focus on cyst wall (c) and slightly lower focus (d). Orientation uncertain. Maximum diameter without processes 46 μm; maximum length processes 10 μm. (e, f) *Echinidinium* sp. B. High focus on cyst wall (e) and slightly lower focus (f). Orientation uncertain. Maximum diameter without processes 45 μm; maximum length processes 8 μm. (g, h) *Echinidinium* sp. C. High focus (g) and low focus (h). Orientation uncertain. Maximum diameter without processes 39 μm; maximum length of processes 8 μm. (i–k) *Lejeunecysta* sp. A. High focus on cingulum (i), slightly lower focus on epicyst (j) and low focus on hypocyst (k). Maximum diameter at cingulum 71 μm. (l–n). *Selenopemphix* sp. A. High focus on epicyst and cingulum (l), slightly lower foci on archeaopyle (m, n). Maximum diameter 90 μm. (o, p) *Trinovantedinium* sp. A. High focus on cingulum (o), slightly lower focus on hypocyst (p) and low focus on ventral surface (q). Maximum diameter at cingulum 87 μm, length of processes 8 μm.

https://doi.org/10.1017/S0016756807004244 Published online by Cambridge University Press

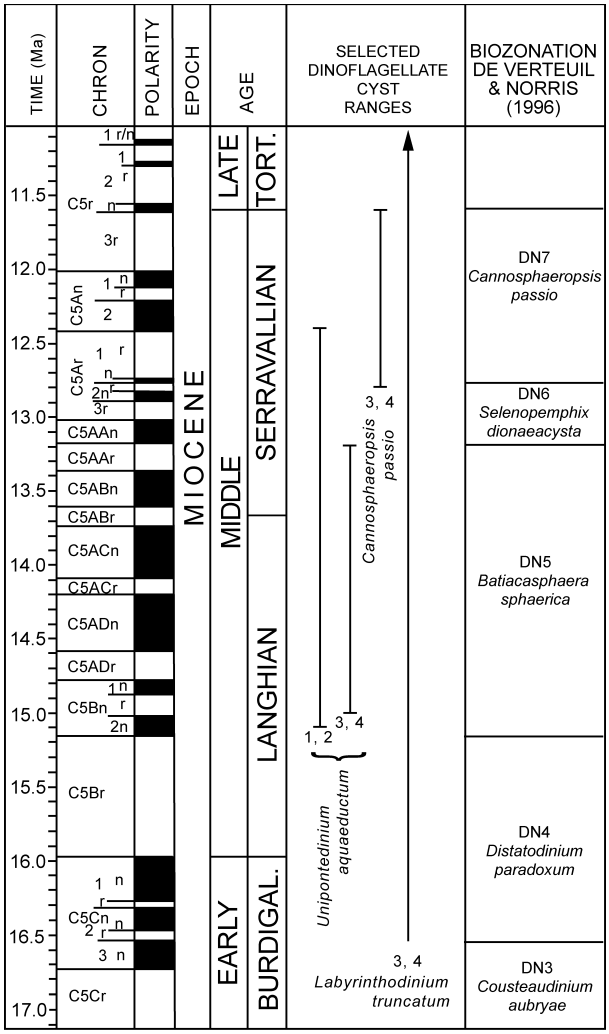

Figure 7. Stratigraphical distribution of selected dinoflagellate cysts in Hole 1318B according to literature: 1 – Zevenboom (1995); 2 – Munsterman & Brinkhuis (2004); 3 – Williams *et al*. (2004); 4 – de Verteuil & Norris (1996). Biozonation according to de Verteuil & Norris (1996).

Zone (DN4: uppermost Lower Miocene to lower Middle Miocene) is defined as the interval from the LO of *Labyrinthodinium truncatum* to the HO of *Distatodinium paradoxum*. *Apteodinium spiridoides* and *Cousteaudinium aubryae* disappear with this zone. The lower boundary, however, is easily defined by the large numbers of *Labyrinthodinium truncatum*, an important dinoflagellate cyst horizon according to de Verteuil & Norris (1996). The *Batiacasphaera sphaerica* Interval Zone (DN5: middle Middle Miocene) is defined as the interval from the HO of *Distatodinium paradoxum* to the HO of *Cleistoaphaeridium placacanthum*. The range of *Unipontedinium aquaeductum* is restricted to this zone. De Verteuil & Norris (1996) consider the LO of *Unipontedinium aquaeductum* as an important dinoflagellate cyst horizon across the North Atlantic and Mediterranean. In the Salisbury Embayment, *Habibacysta tectata* and *Apteodinium tectatum* appear and disappear in the base of this zone, respectively. The *Selenopemphix dionaeacysta* Interval Zone (DN6: upper Middle Miocene) is defined as the interval from the HO of *Cleistophaeridium placacanthum* to the LO of *Cannosphaeropsis passio*. The *Cannosphaeropsis passio* Range Zone (DN7: upper Middle Miocene to uppermost Middle Miocene) holds the entire range of the eponymous species. No other relevant bioevents within this zone are noted.

5.c. The Netherlands

Munsterman & Brinkhuis (2004) presented a biozonation for the Miocene of the Netherlands (southern North Sea Basin). They defined 14 formal dinoflagellate cyst zones and three subzones. No direct calibration of their data through other microfossil biostratigraphy or magnetostratigraphy was provided. However, a number of calibrated dinoflagellate cyst events from the Mediterranean (mainly Zevenboom, 1995) and the Atlantic realm were integrated into their zonal scheme (Fig. 7). Eight zones were defined in the Middle Miocene, based on following dinoflagellate cyst events: LO of *Labyrinthodinium truncatum*, LO and HO of *Unipontedinium aquaeductum*, HO of *Cousteaudinium aubryae*, HO of *Palaeocystodinium ventricosum* (*sensu* Zevenboom, 1995), LO of *Achomosphaera andalousiensis*, HO of *Cerebrocysta poulsenii*, HO of *Cannosphaeropsis poulsenii*. Munsterman & Brinkuis (2004) place the LO of *Labyrinthodinium truncatum* in the North Sea Basin at 15.8 Ma, which is, compared to other biozonations, relatively late. The authors, however, suspect a delayed entry of this species (D. Munsterman, pers. comm.). The LOs of the latter species and *Cerebrocysta poulsenii* coincide in the Netherlands, an event also recorded in our study.

5.d. Other studies

An overview of some key dinoflagellate cyst datums with an estimated correlation to magnetostratigraphy and planktonic foraminifer zones is given by Gradstein, Ogg & Smith (2005). *Labyrinthodinium truncatum* has its LO at the Langhian–Burdigalian boundary, which is placed at 15.97 Ma. The LO of *Unipontedinium aquaeductum* coincides with the HO of *Cousteaudinium aubryae* at 14.9 Ma.

Williams *et al*. (2004) gave an overview of global dinoflagellate cyst events for the Late Cretaceous through the Neogene based on a high-resolution analysis of two sites offshore of Tasmania (ODP Leg 189) and literature data (Fig. 7). The proposed bioevents are calibrated against detailed magnetostratigraphical results from ODP Leg 189. Dinoflagellate cysts events are grouped into low-, mid- and high-latitude associations for both hemispheres.

6. Palaeomagnetic and biostratigraphical dating of Hole U1318B and Hole U1318C

Only the inclination data from the characteristic remanent magnetizations were retained for the interpretation

https://doi.org/10.1017/S0016756807004244 Published online by Cambridge University Press

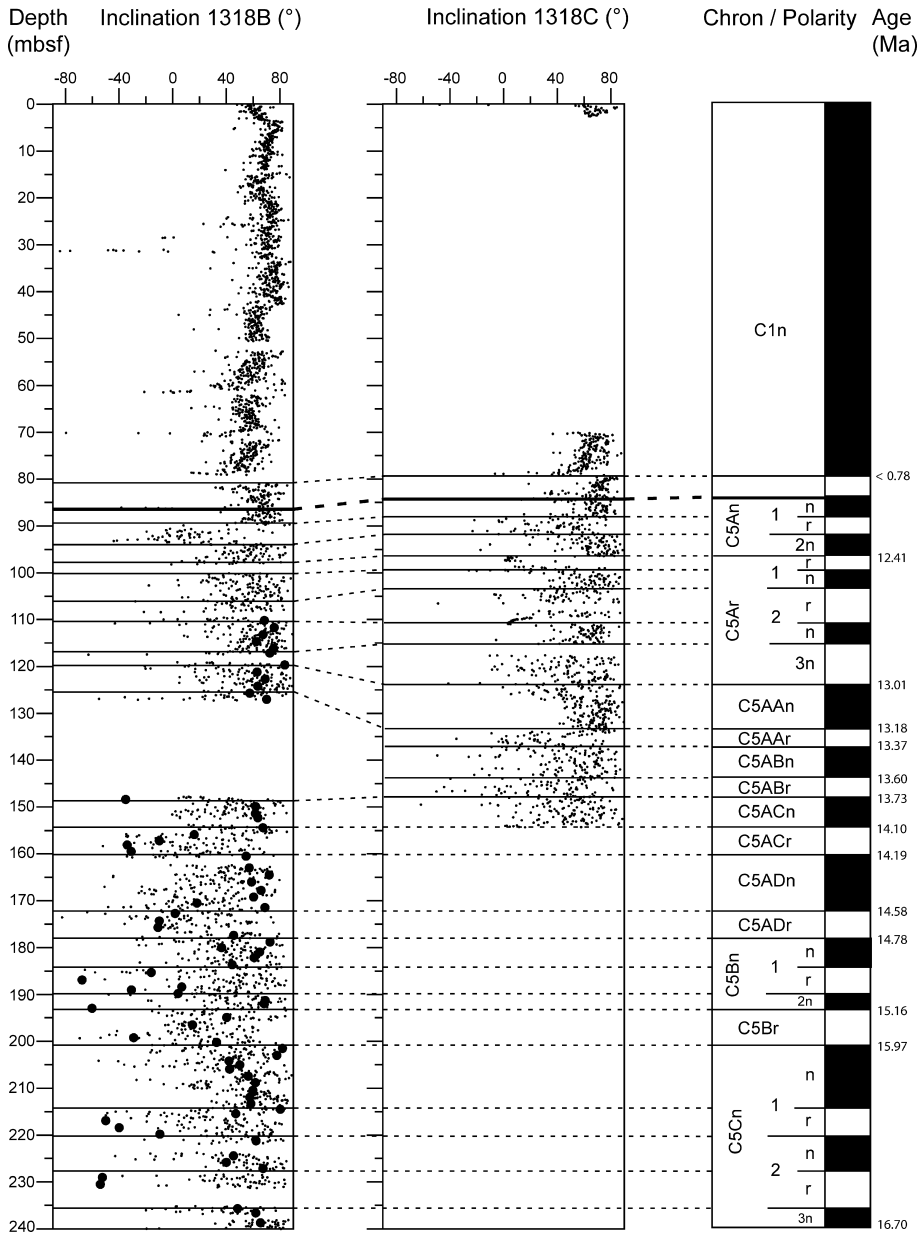

Figure 8. Inclination records at peak fields of 15 mT and interpreted magnetostratigraphical framework in holes U1318B and U1318C. Large dots represent magnetization directions obtained by the standard least-squares method on discrete samples (Kirschvink, 1980). Black horizontal lines represent the interpreted chrons/subchrons.

of a magnetostratigraphical framework (Fig. 8). Magnetostratographical dating was possible by correlating the inclination records with the geomagnetic polarity timescale from Lourens *et al*. (2005) (Table 1).

The inclination data cluster around approximately 66° above 82.0 mbsf and 79.9 mbsf in holes U1318B and U1318C, respectively. Below these depths, inclination data show a small shift, which can be explained by the presence of more reworked and coarser material in the intervals between 82.0 and 86.2 mbsf (Hole U1318B) and 79.9 and 84.2 mbsf (Hole U1318C). The inclinations of the uppermost sections correspond with the reference inclination of the present geomagnetic field at the drilling site, which is 66.36°, according to the International Geomagnetic Reference Field 2005. These positive inclinations can be interpreted as a normal polarity zone corresponding with the Brunhes Chron, which has an age < 0.78 Ma.

Below these depths, inclination data become more scattered. Also, magnetic intensities drop below these depths to low values (Expedition 307 Scientists, 2006). The extremely depleted values of the magnetic intensities in the lowermost sections are greater than can be accounted for by dilution with magnetite-poor sediments and suggest that post-depositional destruction of magnetite has occurred, explaining the scattered directional data at these depths. Florindo, Roberts & Palmer (2003) showed that dissolution of

https://doi.org/10.1017/S0016756807004244 Published online by Cambridge University Press

Table 1 Overview of the chrons and subchrons encountered in holes U1318B and U1318C

Polarity chron/ subchron	Normal polarity interval (Ma)		Epoch, stage (approx.)
	Top	Base	
C1n (Brunhes)	0.000	0.781	Pleistocene
C5An.1n	12.014	12.116	Miocene, Serravalian
C5An.2n	12.207	12.415	Miocene, Serravalian
C5Ar.1n	12.730	12.765	Miocene, Serravalian
C5Ar.2n	12.820	12.878	Miocene, Serravalian
C5AAn	13.015	13.183	Miocene, Serravalian
C5Abn	13.369	13.605	Miocene, Serravalian
C5ACn	13.734	14.095	Miocene, Serravalian
C5ADn	14.194	14.581	Miocene, Serravalian
C5Bn.1n	14.784	14.877	Miocene, Langhian
C5Bn.2n	15.032	15.160	Miocene, Langhian
C5Cn.1n	15.974	16.268	Miocene, Langhian
C5Cn.2n	16.303	16.472	Miocene, Langhian
C5Cn.3n	16.543	16.721	Miocene, Burdigalian

The boundary chron/subchron ages are according to Lourens *et al*. (2005).

magnetite is a common feature in siliceous sedimentary environments, whereby thermodynamic calculations indicate that magnetite is unstable under conditions of elevated dissolved silica concentrations (and appropriate Eh-pH conditions), and predict that magnetite will break down to produce iron-bearing smectite. Pore water analyses in the off-mound sediments indeed show an increase in silica concentrations in the lowermost sections (Expedition 307 Scientists, 2006).

However, a tentative magnetostratigraphical framework can be proposed below 86 mbsf and 84 mbsf for holes U1318B and U1318C, respectively, based on the general inclination trends and taking into account the presence of an important unconformity and some smaller-scaled erosive boundaries (Expedition 307 Scientists, 2006). The unconformity is localized at 86.2 and 84.2 mbsf in holes U1318B and U1318C, respectively, and corresponds with the RD1 moundbase unconformity (Fig. 2). The palynological analysis showed that a latest Middle Miocene age can be proposed for the sediments immediately below the unconformity. This palynological data was used as a palaeomagnetic tiepoint.

Another tiepoint is provided by a Sr-isotope analysis (Kano *et al*. 2007). Although this isotope study focuses on the origin and growth history of Mound Challenger (Hole U1317), some Sr-isotope analysis on skeletal aragonite from bivalves at Site 1318 were performed. The Sr-isotope analysis of a bivalve at a depth of 140.83 mbsf in Hole U1318C (Core 9X, Fig. 3) gives a mean age of 13.38 Ma (12.74 Ma to 14.62 Ma, range of ages from the isotopic value $\pm 2\sigma$ on the upper/lower limit age curve), and confirms the palynological data (Fig. 9).

Figures 8, 9 and Table 1 represent the magnetostratigraphical framework, and the boundary Chron ages according to Lourens *et al*. (2005). The palaeomagnetic analysis indicates an age between late Burdigalian (Chron C5Cn.3n: 16.72 Ma) and late Serravallian at 86 mbsf (C5An.1n: 12.01 Ma) for the sections studied (Table 1, Figs 8, 9).

Unipontedinium aquaeductum has a continuous, but restricted, range in the upper part of the section studied from sections 1318B-17X-3 (lower part of Chron C5Acn, 14.10 Ma) to 1318B-11H-4 (base of Chron C5An.2n, approximately 12.4 Ma) (Figs 4, 9). The higher occurrence of a sole, fragmented specimen is considered not to be *in situ*. Zevenboom (1995) placed the LO of *Unipontedinium aquaeductum* at the Cessole, Italy in the upper part of polarity subchron C5Bn.2n (15.1 Ma following Lourens *et al*. 2005), while the highest common occurrence of *Unipontedinium aquaeductum* at Cassinasco, Italy is located in the basal part of polarity subchron C5An (12.4 Ma following the timescale of Lourens *et al*. 2005). These dates were also used by Munsterman & Brinkhuis (2004) in their southern North Sea dinoflagellate cyst zonation. Williams *et al*. (2004) placed the LO of *Unipontedinium aquaeductum* at 15 Ma, based on data of de Verteuil & Norris (1996). The latter authors gave an overview of the global, non-calibrated LOs and HOs of *Unipontedinium aquaeductum*, in the lower Middle Miocene and the middle Middle Miocene, respectively. Higher stratigraphical occurrences are considered to be reworked.

Cannosphaeropsis passio is continuously recorded in the uppermost part from sections 1318B-12H-1 (base of Chron C5Ar.1r) to 1318B-11H-1 (C5An.1r), and has thus in this study a range from 12.73 Ma to 12.12 Ma (Figs 4, 9). Organic-walled phytoplankton from the uppermost core 1318B-10H, immediately below the unconformity, were not examined in this study, and a slightly younger occurrence might be possible (Figs 4, 9). The HO would then lie in Chron C5An.1n at 12.01 Ma. Many authors consider this species as an index species for the late Middle Miocene (e.g. de Verteuil & Norris, 1996; Munsterman & Brinkhuis, 2004; Strauss, Lund & Lund-Christensen, 2001; Williams *et al*. 2004). According to the latter, *Cannopshaeropsis passio* has a restricted occurrence from 12.8 Ma to the Serravallian–Tortonian boundary, based on records from de Verteuil & Norris (1996). This implies that the considered section has a middle to late Serravallian age. Zevenboom (1995) recorded a single specimen, as *Cannosphaeropsis utinensis*, in the base of the Tortonian in the Mazzapiedi section (Italy), more specifically in the top of subchron C5r, corresponding with an age of approximately 11 Ma (Lourens *et al*. 2005). Munsterman & Brinkhuis (2004) found a similar occurrence above the Serravallian–Tortonian, but did not specify the exact position. Most probably, both findings above the Middle–Upper Miocene boundary can be attributed to reworking.

Both subspecies *Labyrinthodinium truncatum truncatum* and *Labyrinthodinium truncatum modicum* are present through the greater part of the section studied;

https://doi.org/10.1017/S0016756807004244 Published online by Cambridge University Press

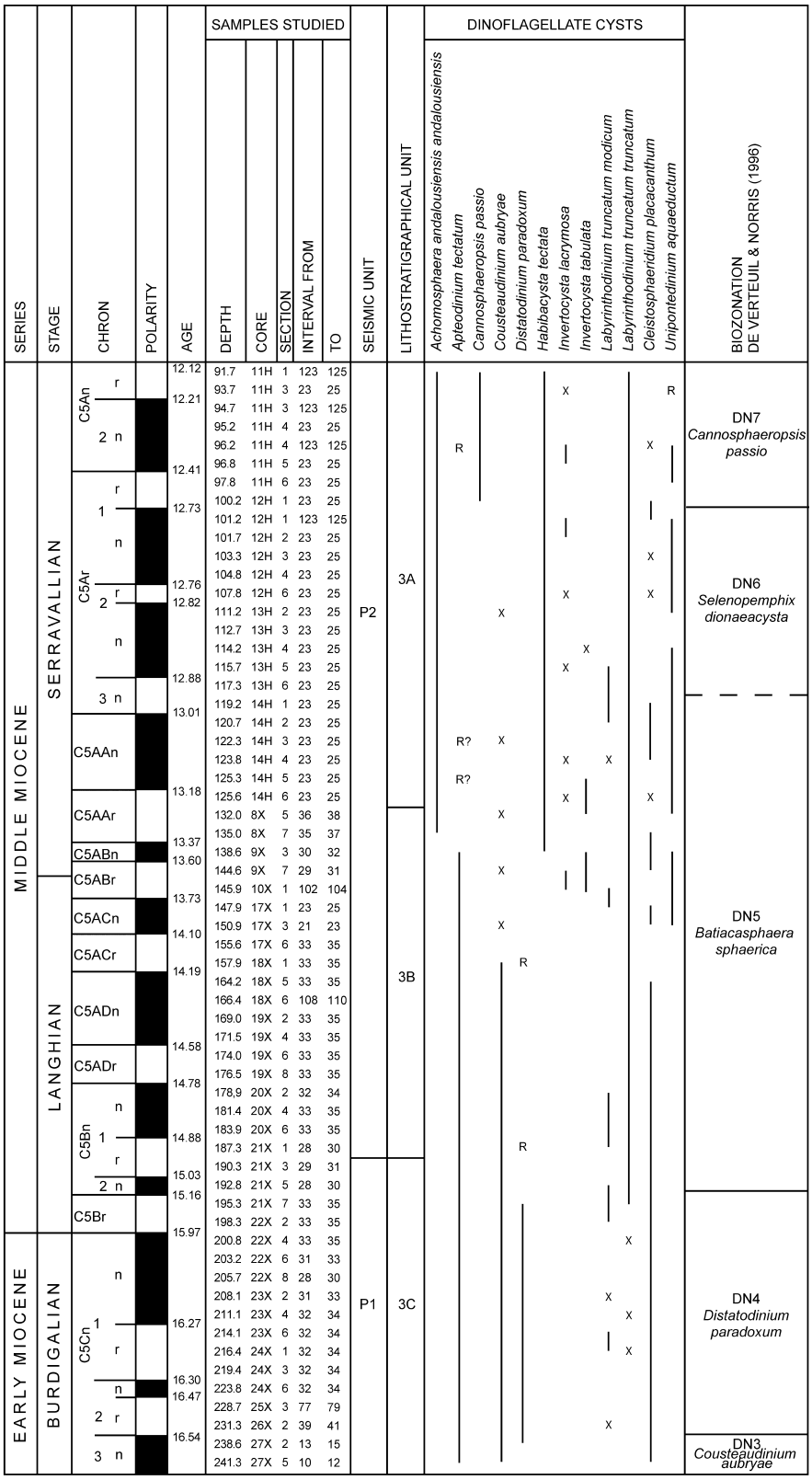

Figure 9. Distribution of selected dinoflagellate cyst in Hole 1318B and Hole 1318C, together with the palaeomagnetic interpretation of the sequence, and biozonation according to de Verteuil & Norris (1996). Solid line – continuous occurrence, X – scattered occurrence; R? – possibly reworked; R – reworked. Dashed horizontal line – uncertain boundary.

they are only absent in lowermost core 1318B-27X. The LO lies in section 1318B-26X-2 in the base of Chron C5Cn.2r at 16.54 Ma (Figs 4, 9). Although many authors place the LO of *Labyrinthodinium truncatum* just below the Burdigalian–Langhian boundary (e.g. de Verteuil & Norris, 1996; Munsterman & Brinkhuis,

https://doi.org/10.1017/S0016756807004244 Published online by Cambridge University Press

2004; Strauss *et al*. 2001), no precise age is specified. Williams *et al*. (2004) located the LO of this species at 16.5 Ma and the HO at 7.85 Ma (late Tortonian), based on the records of de Verteuil & Norris (1996).

The biozonation of de Verteuil & Norris (1996) can readily be applied to the studied sequences (Fig. 9). The *Cousteaudinium aubryae* Interval Zone (DN3: middle Lower Miocene to upper Lower Miocene) is recognized in the two lowermost samples, immediately below the LO of *L. truncatum*. *Apteodinium spiridoides*, a major component of the assemblage in the type area, was not recorded in the Porcupine Basin, while *Cleistosphaeridium placacanthum* is ubiquitous. The *Distatodinium paradoxum* Interval Zone (DN4: uppermost Lower Miocene to lower Middle Miocene) is recognized from sections 1318B-26X-2 to 1318B-21X-7 where the eponymous species has its HO. The recognition of the *Batiacasphaera sphaerica* Interval Zone (DN5: middle Middle Miocene), defined as the interval from the HO of *Distatodinium paradoxum* to the HO of *Cleistosphaeridium placacanthum*, proves difficult. The latter species has its highest continuous occurrence in section 1318B-14H-1, where the upper boundary of this zone could be placed. However, *Unipontedinium aquaeductum*, a species restricted to this zone in the Salisbury Embayment type area, occurs continuously, higher in the studied sequence. Consequently, the location of the upper boundary of the DN5 Zone is unsure and tentatively positioned above section 1318B-14H-1. The *Selenopemphix dionaeacysta* Interval Zone (DN6: upper Middle Miocene) is a 'gap' zone (see Section 5.d). The *Cannosphaeropsis passio* Range Zone (DN7: upper Middle Miocene to uppermost Middle Miocene) is recognized from sections 1318B-12H-1 (123–125) to the top section 1318B-11H-1 (123–126).

In conclusion, palaeomagnetic and biostratigraphical data indicate a late Burdigalian to late Serravallian age for the studied section. An overview of the magnetostratigraphical and biostratigraphical tiepoints versus the depth (mbsf) for holes U1318B and U1318C is presented in Figure 10. Based on the magnetostratigraphical tiepoints, an average sedimentation rate could be calculated of 3.3 cm ka^{-1}. However, this value should be interpreted with care as compaction might have played an important role. The age estimates from magnetostratigraphy and biostratigraphy are in broad agreement; both suggest ages from late Burdigalian to late Serravallian.

An early to middle Langhian to late Serravallian age can be attributed to seismic unit P2. The seismic discontinuity RD2, separating seismic units P1 and P2, and lithostratigraphical units 3C and 3B, most probably represents a hiatus of minor magnitude since it is not readily reflected as a major shift in the dinoflagellate cyst assemblage. The location of the boundary between biozones DN4 and DN5 a few metres below the discontinuity might be a reflection

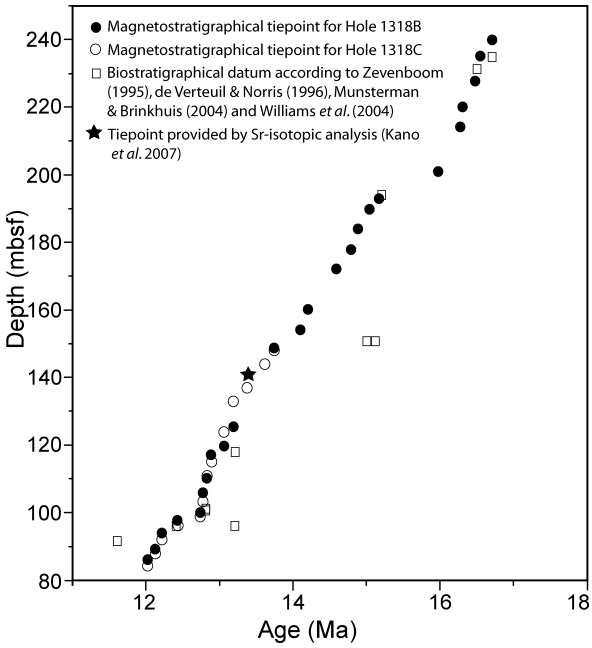

Figure 10. Age (Ma) versus depth (mbsf) for palaeomagnetic, biostratigraphical and isotopic tiepoints at Site U1318.

of this hiatus. The detailed lithological analysis of the cores does not provide more information on this discontinuity, and further study is thus needed. Only a broad late Burdigalian to early Langhian age can be proposed for the upper part of seismic unit P1.

The youngest sediments in the sequence studied are thus of late Serravallian age, and it remains unknown whether the unconformity RD1 located at the top of the section studied is precisely located at the Serravallian–Tortonian boundary or in the uppermost Serravallian. Nevertheless, a correlation of the upper boundary of the section studied, that is, the unconformity in core 10H, can be proposed with the major sequence boundary Ser4/Tor1 at 10.5 Ma (Hardenbol *et al*. 1998).

7. Palaeoenvironmental indices

The composition of a fossil dinoflagellate cyst assemblage is largely determined by the palaeoenvironment. Parameters such as temperature, salinity and nutrient availability influence the contemporanous assemblage and thus also the fossil assemblage. However, numerous factors interfere with an interpretation of a fossil assemblage in terms of past environments. A thorough review of the history of palaeoecological studies with dinoflagellate cysts and its restrictions was given by Dale & Dale (2002). One of the main limiting factors in the Porcupine Basin for a reconstruction of the Miocene palaeoenvironment based on dinoflagellate cysts is the location of the drill site. Hole U1318B was drilled at a depth of 420 m and the site can be considered as located on the upper slope. Considering this depth, it is clear that site U1318B has known an oceanic influence since early Neogene times, since no

https://doi.org/10.1017/S0016756807004244 Published online by Cambridge University Press

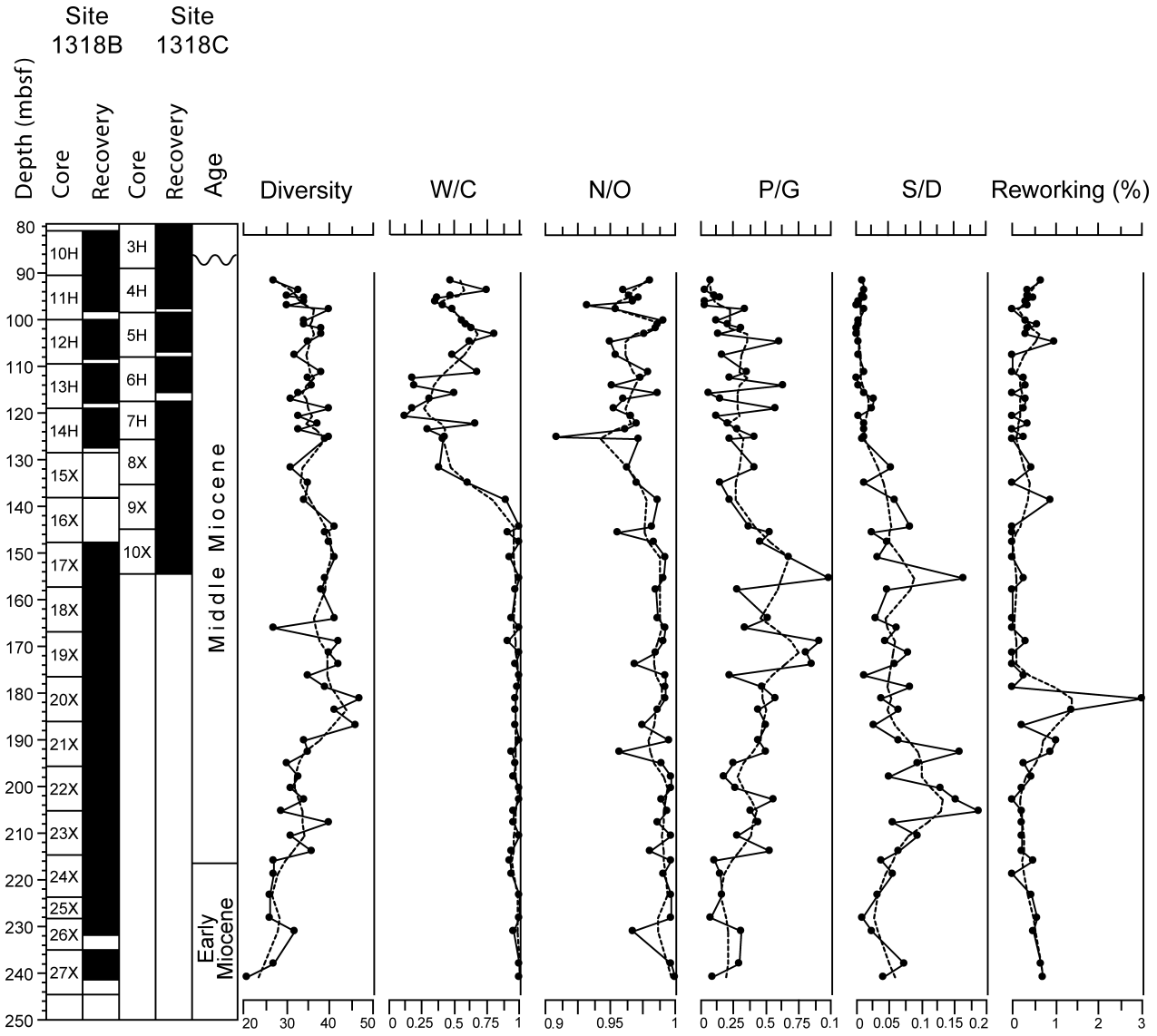

Figure 11. Diversity, reworking and ratios in holes 1318B and 1318C. The position of the samples is given, together with the stratigraphical position. Dashed line – smooth curve.

elements in the sedimentological or palaeontological record point to a neritic, shelfal environment. A truly neritic fossil assemblage does not contain any oceanic species such as *Impagidinium* spp., but on the other hand, an assemblage from the oceanic realm or continental slope contains not only true oceanic species, but also many neritic species transported from the shelf to the upper slope depositional area (Dale, 1996; Dale & Dale, 1992, 2002). In this respect, a local palaeoenvironmental reconstruction is limited at drill site U1318B, but a regional range for the palaeoenvironmental indices covering not only the Porcupine Basin but the southwestern Irish shelf is assumed.

7.a. Diversity

The diversity index represents the number of dinoflagellate cysts species recorded in one sample; other marine palynomorphs were not included in the diversity index (Fig. 11).

7.b. Temperature signal

Several authors have proposed proxies for reconstructions of the variation in sea-surface temperature, the so-called W/C ratios. In his detailed palynological study of the Pliocene MIS M2 cooling event in DSDP Hole 610 (Rockall Trough, eastern North Atlantic), S. De Schepper (S. De Schepper, unpub. Ph.D. thesis, Cambridge Univ. 2006) gave an extensive overview of the species used in several warm/cold indices proposed by Boessenkool *et al*. (2001), Marret & Zonneveld (2003), Versteegh & Zonneveld (1994) and Warny (S. Warny, unpub. Ph.D. thesis, Univ. Catholique de Louvain, 1999). The W/C ratio is usually calculated as $nW/(nW + nC)$ with n the number of specimens counted, W representing the warm-water indicating species and C the cold-water indicating species (Fig. 11). Different species were used by these authors for the establishment of the temperature

https://doi.org/10.1017/S0016756807004244 Published online by Cambridge University Press

signal. Versteegh (1994) stated that the choice of certain species depends on environmental factors, and it is conceivable that the temperature signal is an expression of ecological factors. De Schepper (S. De Schepper, unpub. Ph.D. thesis, Cambridge Univ. 2006) constructed W/C curves according to the above-mentioned authors and calculated the correlation of the W/C curves with a $\delta^{18}O$ isotopic curve of the MIS M2 interval from DSDP Hole 610A. The R^2 values vary between 0.3427 (Boessenkool *et al*. 2001) and 0.5673 (S. Warny, unpub. Ph.D. thesis, Univ. Catholique de Louvain, 1999). Based on published data and the data from DSDP Hole 610A, De Schepper (S. De Schepper, unpub. Ph.D. thesis, Cambridge Univ. 2006) considers *Impagidinium aculeatum*, *Impagidinium patulum*, *Impagidinium strialatum*, *Melitasphaeridium choanophorum*, *Selenopemphix nephroides*, *Spiniferites hyperacanthus* and *Spiniferites mirabilis* as warm-water species, and *Bitectatodinium tepikiense*, *Filisphaera filifera* and *Impagidinium pallidum* as cold-water species. The curve obtained with these species gives a R^2 value of 0.6686 with the $\delta^{18}O$ isotopic curve.

Lingulodinium machaerophorum, Polysphaeridium zoharyi, Tuberculodinium vancampoae and *Operculodinium israelianum* are species with an affinity for equatorial–temperate waters (Dale, 1996). Head (2003) suggests a warm-water association for *Nannobarbophora gedlii*. *Impagidinium paradoxum*, *Impagidinium patulum* and *Impagidinium strialatum* are also considered to be temperate to tropical species (Marret & Zonneveld, 2003), while *Tectatodinium pellitum* may be regarded as a subtropical to tropical coastal species. Head (1997) regards *Melitasphaeridium choanophorum* as a good indicator for relatively warm surface waters. According to Head (1993), the distribution of the genus *Sumatrodinium* suggests affinities with tropical and subtropical to warm temperate waters. Dale (1996) considers *Bitectatodinium tepikiense* and *Impagidinium pallidum* as species characteristic for the subpolar zone. On the basis of its fossil occurrences, Head, Norris & Mudie (1989*c*) and Head (1994) assume that high numbers of *Habibacysta tectata* indicate cool conditions. Versteegh (1994) also considers *Habibacysta tectata* as a cool-water species.

Given the close location to DSDP Hole 610A, the selection by De Schepper (S. De Schepper, unpub. Ph.D. thesis, Cambridge Univ. 2006) of warm-water and cold-water indicating species was followed, supplemented with *Impagidinium paradoxum, Lingulodinium machaerophorum, Nannobarbophora gedlii*, *Operculodinium israelianum*, *Polysphaeridium zoharyi, Sumatradinium druggii, Sumatradinium soucouyantiae*, *Sumatradinium hamulatum*, *Tectatodinium pellitum* and *Tuberculodinium vancampoae* as warm-water indicating species and *Bitectatodinium tepikiense*, *Filisphaera filifera*, *Impagidinium pallidum* and *Habibacysta tectata* as cold-water species.

7.c. Neritic/Oceanic signal and terrestrial influence

An index relying on the ratio between neritic and oceanic species does not represent the distance of the depositional area from the coastline, but is a proxy for the degree of transport of neritic species from the shelf to the ocean, or as a measure for the changes of the neritic water mass influence in the depositional area (Versteegh, 1994). The ratio is calculated as $N/O = nN/(nN + nO)$, with n the number of specimens counted, N representing the neritic species and O the truly oceanic species (Fig. 11).

According to Dale (1996), species of the genus *Impagidinium* are considered to be oceanic, while representatives of the genus *Nematosphaeropsis* have neritic–oceanic affinties. In their ecological overview of the geographical distribution of dinoflagellate cysts, Marret & Zonneveld (2003) regard *Polysphaeridinium zoharyi, Selenopemphix nephroides, Tectatodinium pellitum* and *Tuberculodinium vancampoae* as neritic cysts. *Habibacysta tectata* and species of *Sumatradinium* spp. are considered to be neritic species by Head (1993, 1994). De Schepper (S. De Schepper, unpub. Ph.D. thesis, Cambridge Univ. 2006) considers *Edwardsiella sexispinosum* as an oceanic species. *Apteodinium* spp., *Dapsilidinium* spp., *Lingulodinium machaerophorum* and *Systematophora* are also thought to reflect marginal marine conditions (Zevenboom, Brinkhuis & Visscher, 1994). The boundary between both realms is inhabited by *Operculodinium centrocarpum* (Dale, 1996). In addition to the above mentioned species, De Schepper (S. De Schepper, unpub. Ph.D. thesis, Cambridge Univ. 2006) considers *Achomosphaera andalousiensis andalousiensis*, *Bitectatodinium tepikiense*, *Bitectatodinium*? *serratum*, *Invertocysta lacrymosa*, *Melitasphaeridium choanophorum*, *Operculodinium*? *eirikianum*, *Selenopemphix dionaeacysta*, the *Spiniferites*/*Achomosphaera* spp. Group and *Trinovantedinium glorianum* as neritic species.

7.d. Productivity signal

Eutrophic or nutrient-rich marine environments are often characterized by a high primary productivity of phytoplankton. The nutrients are brought to deep shelfal areas by upwelling watermasses and to coastal areas by river discharge. Phytoplankton associations in such areas are often dominated by diatoms, although dinoflagellates are usually present, though in much lower numbers (Dale, 1996). Protoperidinioid dinoflagellates favour these areas because of the presence of abundant prey. Dale (1996) reviews dinoflagellate cyst studies in upwelling areas and underlines the importance of protoperidinioid dinoflagellates as a primary signal for upwelling. Their abundance versus gonyaulacoid cysts is considered as a proxy for palaeoproductivy. Reichart & Brinkhuis (2003) demonstrated the positive correlation between absolute

abundance of protoperinioid cysts and upwelling. Although protoperidiniod dinoflagellate cysts are sensitive to aerobic decay (Zonneveld, Versteegh & de Lange 2001), Reichart & Brinkhuis (2003) further showed that the principal trends in the number of protoperidinioid cysts per gram of sediment do not alter significantly after intense oxidation. Their presence, or sometimes dominance, in every sample of this study, suggests that post-depositional oxidation did not alter the assemblages. Protoperidinioid dinocysts with brown, smooth walls, rounded outlines and indications of an archeopyle are grouped as 'Round brown cysts' (Fig. 4). These include mostly species of the genus *Brigantedinium*. Representatives of the genera *Lejeunecysta*, *Selenopemphix* and *Trinovantedinium* are cysts produced by heterotrophic dinoflagellates living on the inner shelf, and may represent upwelling (Reichart & Brinkhuis, 2003). However, the oceanic species *Impagidinium paradoxum* and the outer neritic to oceanic *Nematosphaeropsis labyrinthus*, clearly indicate the influence of oligotrophic (oceanic) water masses (Dale, 1996). The P/G ratio is calculated as nP/(nP + nG) with n the number of specimens counted, P reprensenting peridinioid cysts (round brown cysts, *Echinidinium* spp., *Lejeunecysta* spp., *Sumatradinium* spp. and *Trinovantedinium* spp.) and G representing all other dinoflagellate cysts excluding the goniodomacean *Tuberculodinium vancampoae* and *Geonettia*? sp. ind., the polykrikacean *Polykrikos* and the organic membranes of calcareous cysts (Fig. 11).

7.e. Terrestrial or continental influence

According to Versteegh (1994), the ratio between the sporomorphs (spores and pollen) and the marine palynomorphs is a measure for the terrestrial influence versus the marine influence and in this manner is a measure for the distance between the depositional area and the coast. Site U1318B is located approximatively 100 km from the present-day coastline and, as already mentioned, is located on the upper slope. It is unsurprising that the greater part of the terrestrial palynomorphs consist of bisaccate pollen brought into the depositional area by wind. Non-bisaccate pollen and spores are rare. The ratio is calculated as S/D = nS/(nS + nD) with n the number of specimens counted, S representing pollen and spores, and D dinoflagellate cysts and acritarchs (Fig. 11). We assume that the majority of the pollen and spores are primarily transported by wind rather than by rivers, since most pollen are bisaccate and of the *Pinus* type. The high percentage of bisaccate pollen in our dataset may be overrepresented in marine sediments because of their high buoyancy (Traverse, 1988).

7.f. Reworking

The reworking is given as the relative proportion to the *in situ* marine palynomorphs (Fig. 11). The amount of reworked dinoflagellate cysts and other palynomorphs is indicative of sea-level variations (Sturrock, 1996).

8. Palaeoenvironmental considerations

The dinoflagellate cyst assemblages are diverse and comprise species with different ecological preferences. Species with oceanic preferences such as *Impagidinium* spp. and *Nematosphaeropsis* sp. are present in every sample, although they never dominate the assemblage. *Unipontedinium aquaeductum*, here considered as an outer neritic species because of its absence in shallow marine environments (de Verteuil & Norris, 1996), is distinctly present. The majority of the species can be considered as neritic, while truly shallow marine species such as *Lingulodinium machaerophorum* and *Polysphaeridium zoharyi* are present to rare. Considering the location of Hole U1318B on the upper slope at a depth of 420 m, the dominance of these neritic species confirms the transport of truly neritic species from the shelfal area to the deeper depositional area.

Between the base of the studied sequence at 241 mbsf (core 1318B-27X) to approximately 144 mbsf (section 1318B-9X-7), the warm/cold ratio (Fig. 11) ranges between 0.9 and 1, and indicates a dominance of thermophilic dinoflagellate cyst species. Around 139 mbsf (section 1318B-9X-3), a distinct drop to values lower than 0.5 is observed, reflecting a distinct increase of cold-water indicating dinoflagellate cysts over approximately 35 m, followed by a short return of warm-water indicating species. This sudden shift at 139 mbsf is also indicated by the other ratios, although to a lesser degree. The S/D ratio (the expression of the continental influence) plunges towards values below 0.01. The productivity signal (the P/G ratio) and the neritic signal (the N/O ratio) both decrease slightly; this is caused by a decrease in protoperidinioid cysts and an increase in oceanic cysts, respectively.

Throughout the studied section, the dinoflagellate cyst diversity is considered relatively high, between 30 and 40 species per sample. The reworking remains low at values below 2 %, although an abrupt influx of allochtonous elements, coupled with a rise in dinoflagellate cyst diversity, in core 20X at 180 mbsf is observed. Reworking tends to be higher during periods of low sea-level and lower during periods of high sea-level. Low sea-levels cause the river base level of erosion to lower, which results in higher amounts of terrestrial derived organisms and reworked fossil assemblages from the continent transported to the sea.

9. Discussion and conclusion

During the latest Oligocene, a warm phase was established during which the extent of the Antarctic ice sheets reduced and the temperature of bottom water increased. This warming period culminated in

https://doi.org/10.1017/S0016756807004244 Published online by Cambridge University Press

the Middle Miocene Climatic Optimum, which is well documented in the marine and continental realm from several proxies and lasted approximately from 17 to 14.5 Ma (Böhme, 2003; Zachos *et al*. 2001). A gradual global cooling phase set in after 14.5 Ma and was characterized by several short-lived glaciations, the so-called Mi-isotope zones Mi3, Mi4, Mi5 and Mi6 of Miller *et al*. (1991), with a maximum age of 13.7, 12.9, 11.9 and 10.3 Ma, respectively (Miller *et al*. 1998). Distinct excursions in a $\delta^{18}O$ curve, based on a benthic stable isotope record from the southeast Atlantic (ODP Site 1085), are dated at 13.8, 13.2, 11.7 and 10.4 Ma and correlated by Westerhold, Bickert & Rohl (2005) to the Mi3, Mi4, Mi5 and Mi 6 events of Miller *et al*. (1991) and Miller *et al.* (1998). The stepwise cooling during the Middle Miocene climatic transition is further documented by Shevenell, Kennett & Lea (2004) and Abels *et al*. (2005), who consider Mi3a at 14.2 Ma a minor step in the cooling phase and Mi3b at about 13.8 Ma a major step. Based on Mg/Ca data from planktonic foraminifers, Shevenell, Kennett & Lea (2004) assume sea-surface temperature cooled 6 to 7 °C during the Middle Miocene climate transition in the southwest Pacific. The astronomical forcing by long-period orbital cycles is considered to be the driving factor behind the Neogene climate changes (Zachos *et al*. 2001). Based on integrated stratigraphy and astronomical tuning of a middle Miocene sequence in Malta, Abels *et al*. (2005) demonstrated that the major cooling step at 13.82 ± 0.03 Ma coincides with minimum eccentricity values associated with the 400 ka cycle and minimum obliquity amplitudes of the 1.2 Ma cycle. The observed temperature drop (Fig. 11) can be paralleled with the onset of the global, climatic cooling phase which occurred after the Middle Miocene Climatic Optimum. The relative dating (see Section 6) places the distinct cooling event at 139 mbsf in Chron C5Bn at approximately 13.60 Ma, and suggests a correlation with the Mi3 event of Miller *et al*. (1998).

The sea-level fall associated with the Middle Miocene climatic transition shows a considerable geographical variability. $\delta^{18}O$ data from the Marion Plateau (off NE Australia) indicate a sea-level fall of 50.0 ± 5.0 m (John, Karner & Mutti, 2004), while a multidisciplinary study on the New Jersey continental slope indicates a sea-level drop of 25 m $\pm$ 5 m (Miller *et al*. 1998). According to Westerhold, Bickert & Rohl (2005), the sea-level drop in the southeast Atlantic associated with the cooling during the late Middle Miocene is estimated at 43 m. Based on a multidisciplinary study of the New Jersey continental platform, Miller *et al.* (1998) demonstrate a good correlation between sequence boundaries and increases of $\delta^{18}O$, and postulate the expansion of ice sheets since about 42 Ma to be the main controlling factor on formation of sequence boundaries. Given the location of Site U1318B and the depth of the present-day sea-floor at 420 m, it is unlikely that the sea-level lowering will significantly influence the dinoflagellate cyst associations. The neritic/oceanic signal (Fig. 11) points to an increase of oceanic, oligothropic species and a reduction of the neritic species. The latter would then implicate a reduction of the downslope transport of neritic dinoflagellate cysts to the depositional area, which is unusual. Westerhold, Bickert & Rohl (2005) note a distinct enhancement of the transport of shelf-derived terrigenous matter during periods of cooling linked to increased ice-sheet growth on Antarctica. However, the lowering of the productivity together with the increase in oceanic, and thus oligothrophic, species in the Porcupine Basin rather points to a reduction or perhaps even to a shutdown of the upwelling after 14 Ma. At the same time, a collapse of the opal deposition in the North Atlantic realm is observed (Cortese *et al*. 2004). According to these authors, the waxing of the Antarctic glaciers and the development of the North Atlantic Deep Water influenced positively the fractionation of nutrients coupled to the establishment of an anti-estuarine circulation (exchange of deep, nutrient-rich waters for surface, nutrient-poor waters) in the North Atlantic. This circulation impeded the upwelling of silica-rich Antarctic Bottom Water in the North Atlantic.

A reconstruction of the Miocene depositional history based on the dinoflagellate cyst analysis partly confirms the interpretation of Van Rooij *et al*. (2003). Seismic unit P1 was deposited in a relatively calm environment during the later part of the Early Miocene and the earlier part of the Middle Miocene, although upslope-migrating sediment waves suggest the presence of bottom current flow (Fig. 12). Unconformity RD2 is genetically related to the introduction of Norwegian sea water in the North Atlantic (van Rooij *et al*. 2003). Dinoflagellates indicate that this event took place during early Middle Miocene times. The hiatus associated with the unconformity is probably of minor magnitude and as such is not reflected by a clear break in the palynological record. The subsequent deposition of the acoustically transparent unit P2 then took place during the remainder of Middle Miocene times. Reflector RD1 terminates the Middle Miocene sequence, and reflects a basin-wide erosional event deeply affecting units P2 and P1. The unconformity can be dated as terminal Middle Miocene or earliest late Miocene, and correlated with sequence boundary Ser4/Tor1 at 10.5 Ma of Hardenbol *et al*. (1998). Seismic unit P3 is younger than 0.78 Ma and is thus of Middle Pleistocene or younger age.

The Neogene megasequences of the NW European Atlantic margin are bounded by regional unconformities, preserved in the shelfal deposits and continuing into the deep water basins (Stoker *et al*. 2005). It is clear that eustatic sea-level changes cannot account solely for the observed stratal geometry, and unconformities, along the northwestern Atlantic margin, and these authors

https://doi.org/10.1017/S0016756807004244 Published online by Cambridge University Press

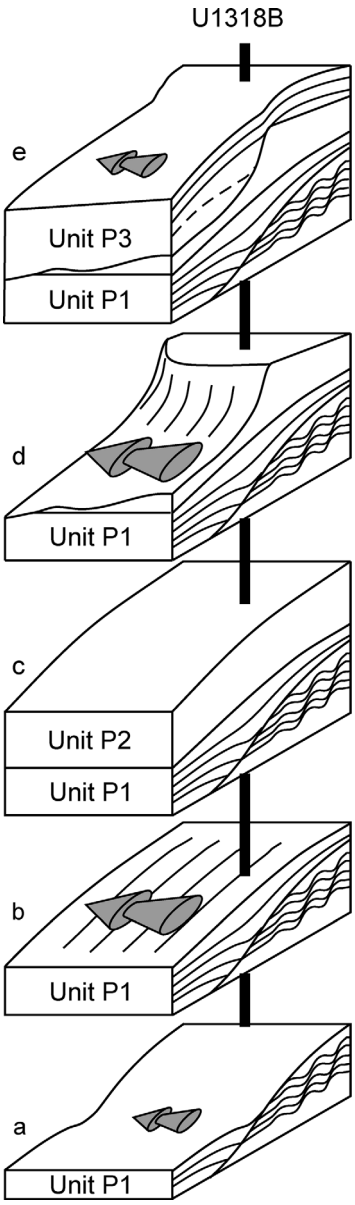

Figure 12. Depositional history in the Belgica mound province. (a, b) Deposition of seismic Unit P1 and formation of sediment waves during Early Miocene and early Middle Miocene times. Subsequent formation of unconformity RD2 during early Middle Miocene times. (c) Deposition of the acoustically transparent Unit P2 during Middle Miocene times and subsequent erosion (unconformity RD1) (d). (e) Deposition of seismic Unit P1 during post-Middle Miocene times. The direction and size of the grey-shaded arrows illustrate the direction and vigour of the bottom currents, allowing drift deposition when small and erosive when large.

point out that middle to late Cenozoic tectonic activity plays a major role in the regional sedimentary and oceanographic dynamics.

Acknowledgements. Prof. Dr Joseph Hus is thanked for the use of the palaeomagnetic measure infrastructure at the Geophysical Centre of the Royal Meteorological Institute in Dourbes and for his excellent support during the measurements. Yuji Fuwa, Klayton Curtis, Margaret Hastedt and Trevor Williams are thanked for their palaeomagnetic help aboard the *JOIDES Resolution* during IODP expedition Leg 307. The authors would like to thank the IODP and Transocean crews and the scientific staff of the *JOIDES Resolution* on IODP Expedition Leg 307. The IODP staffs at the Bremen Core Repository and at Texas A&M University in College Station are thanked for their support during the post-cruise sampling activities. A part of this study has been carried out under the framework of the FWO Genesis and ESF Moundforce project. A. Foubert is a Ph.D. student funded through a FWO-fellowship. D. Van Rooij is a post-doctoral fellow of the FWO Flanders. The discussions with Jan De Coninck on dinoflagellate cyst taxonomy and morphology are appreciated. Jean-Pierre Henriet (Renard Centre of Marine Geology, Ghent University) introduced the first author to the Porcupine Basin and its intriguing geology. His interest and co-operation are kindly acknowledged. The careful reviews by J. Riding (British Geological Survey) and an anonymous reviewer are appreciated. Sabine Vancauwenberghe (Research Unit Palaeontology, Ghent University) is kindly thanked for her technical assistance during palynological maceration.

References

ABELS, H. A., HILGEN, F. J., KRIJGSMAN, W., KRUK, R. W., RAFFI, I., TURCO, E. & ZACHARIASSE, W. J. 2005. Long-period orbital control on middle Miocene global cooling: Integrated stratigraphy and astronomical tuning of the Blue Clay Formation on Malta. *Paleoceanography* **20**(4), 1–17.

BOESSENKOOL, K. P., BRINKHUIS, H., SCHONFELD, J. & TARGARONA, J. 2001. North Atlantic sea surface temperature changes and the climate of western Iberia during the last deglaciation: a marine palynological approach. *Global and Planetary Change* **30**(1), 33–9.

BÖHME, M. 2003. The Miocene Climatic Optimum: evidence from ectothermic vertebrates of Central Europe. *Palaeogeography, Palaeoclimatology, Palaeoecology* **195**(3–4), 389–401.

BROWN, S. & DOWNIE, C. 1984. Dinoflagellate cyst stratigraphy of Paleocene to Miocene sediments from the Goban Spur (Sites 548–550, Leg 80). In *Initial Reports of the Deep Sea Drilling Project, vol. 80* (eds P. C. de Graciansky & C. W. Poag), pp. 643–51. Washington D.C.: U. S. Government Printing Office.

CORTESE, G., GERSONDE, R., HILLENBRAND, C.-D. & KUHN, G. 2004. Opal sedimentation shifts in the World Ocean over the last 15 Myr. *Earth and Planetary Science Letters* **224**, 509–27.

COSTA, L. I. & DOWNIE, C. 1979. Cenozoic dinocyst stratigraphy of Sites 403 to 406 (Rockall Plateau), IPOD, Leg 48. In *Initial reports of the Deep Sea Drilling project* (eds L. Montadert & D. G. Robert), pp. 513–29. Washington D.C.: U.S. Government Printing Office.

DALE, A. L. 1996. Chapter 31. Dinoflagellate cyst ecology: Modelling and geological applications. In *Palynology: Principles and applications, vol. 3* (eds J. Jansonius & D. C. McGregor), pp. 1249–75. AASP (American Association of Stratigraphic Palynologists) Foundation.

DALE, A. L. & DALE, B. 1992. Dinoflagellate contributions to the sediment flux in the Nordic Seas. *Ocean Biocoenosis Series* **5**, 45–76.

DALE, B. & DALE, A. 2002. Environmental application of dinoflagellate cysts and acritarchs. In *Quaternary*

https://doi.org/10.1017/S0016756807004244 Published online by Cambridge University Press

environmental micropalaeontology (ed. S. K. Haslett), pp. 207–24. London: Arnold.

DE GRACIANSKY, P. C., POAG, C. W., CUNNINGHAM, R., LOUBERE, P., MASSON, D. G., MAZZULLO, J. M., MONTADERT, L., MÜLLER, C., OTSUKA, K., REYNOLDS, L. A., SIGAL, J., SNYDER, S. W., VAOS, S. P. & WAPLES, D. 1985. Site 548. In *Initial Reports of the Deep Sea Drilling Project, vol. 80* (eds P. C. de Graciansky, C. W. de Poag, R. Cunningham, P. Loubere, D. G. Masson, J. M. Mazzullo, L. Montadert, C. Müller, K. Otsuka, L. A. Reynolds, J. Sigal, S. W. Snyder, S. P. Vaos & D. Waples), pp. 33–122. Washington D.C.: U.S. Government Printing Office.

DE MOL, B., VAN RENSBERGEN, P., PILLEN, S., VAN HERREWEGHE, K., VAN ROOIJ, D., MCDONNELL, A., HUVENNE, V., IVANOV, M., SWENNEN, R. & HENRIET, J.-P. 2002. Large deep-water coral banks in the Porcupine Basin, southwest of Ireland. *Marine Geology* **188**, 193–231.

DE VERTEUIL, L. 1996. Data report: Upper Cenozoic dinoflagellate cysts from the continental slope and rise off New Jersey. In *Proceedings of the Ocean Drilling program, Scientific Results, vol. 150* (eds J. S. Mountain, K. G. Miller, P. Blum, C. W. Poag & D. C. Twitchell), pp. 439–54. College Station, Texas.

DE VERTEUIL, L. 1997. Palynological delineation and regional correlation of lower through upper Miocene sequences in the Cape May and Atlantic City boreholes, New Jersey coastal plain. In *Proceedings of the Ocean Drilling Program, Scientific Results, vol. 150* (eds K. G. Miller & S. W. Snyder), pp. 129–45. College Station, Texas.

DE VERTEUIL, L. & NORRIS, G. 1996. Miocene dinoflagellate stratigraphy and systematics of Maryland and Virginia. *Micropaleontology* **Supplement 42**, 1–172.

EDWARDS, L. 1984. Miocene dinocysts from Deep Sea Drilling Project Leg 81, Rockall Plateau, eastern North Atlantic Ocean. In *Initial Reports of the Deep Sea Drilling Project, vol. 81* (eds D. G. Robert & D. Schnitker), pp. 581–94. Washington D.C.: U. S. Government Printing Office.

EXPEDITION 307 SCIENTISTS. 2006. Site U1318. In *Proceedings of the Integrated Ocean Drilling program, vol. 307* (eds T. G. Ferlman, A. Kano, T. Williams, J.-P. Henriet & thede Expedition 307 Scientists), pp. 1–57. Washington, D. C.

FENSOME, R. A. & WILLIAMS, G. L. 2004. *The Lentin and Williams Index of Fossil Dinoflagellates 2004 Edition*. AASP (American Assoication of Stratigraphic Palynologists Foundation) Contributions Series no. 42, 1–909.

FLORINDO, F., ROBERTS, A. P. & PALMER, M. R. 2003. Magnetite dissolution in siliceous sediments. *Geochemistry, Geophysics and Geosystems* **4**, 1053.

FOUBERT, A., BECK, T., WHEELER, A.J., OPDERBECKE, J., GREHAN, A., KLAGES, M., THIEDE, J., HENRIET, J. P. & THE POLARSTERN ARK-XIX/3a SHIPBOARD PARTY. 2005. New view of the Belgica Mounds, Porcupine Seabight, NE Atlantic: preliminary results from the Polarstern ARK-XIX/3a ROV cruise. In *Cold-water corals and ecosystems* (eds A. Freiwald & J. M. Roberts), pp. 403–15. Berlin Heidelberg: Springer-Verlag.

GRADSTEIN, F. M., OGG, J. G. & SMITH, A. G. 2005. *A Geologic Time Scale 2004*. Cambridge: Cambridge University Press, 589 pp.

HARDENBOL, J., THIERRY, J., FARLEY, M. B., JACQUIN, T., DE GRACIANSKY, P. C. & VAIL, P. R. 1998. Cenozoic sequence biochronostratigraphy. In *Mesozoic and Cenozoic Sequence Stratigraphy of European Basins* (eds P. C. de Gradiansky, J. Hardenbol, T. Jacquin & P. Vail). Chart 2. SEPM Special Publication no. 60. Tulsa, Oklahoma: SEPM (Society Economic Paleontologists and Mineralogists).

HEAD, M. J. 1993. Dinoflagellates, sporomorphs, and other palynomorphs from the upper Pliocene St. Erth Beads of Cornwall, Southwestern England. *Journal of Paleontology* **67**(3), 1–62.

HEAD, M. J. 1994. Morphology and paleoenvironmental significance of the Cenozoic dinoflagellate genera *Tectatodinium* and *Habibacysta*. *Micropaleontology* **40**, 289–321.

HEAD, M. J. 1997. Thermophilic dinoflagellate assemblages from the Mid Pliocene of Eastern England. *Journal of Palaeontology* **71**(2), 165–93.

HEAD, M. J. 2003. Neogene occurrences of the marine acritarch genus *Nannobarbophora* Habib and Knapp, 1982 Emend., and the new species *Nannobarbophora gedlii*. *Journal of Paleontology* **77**(2), 382–5.

HEAD, M. J., NORRIS, G. & MUDIE, P. 1989*a*. Palynology and dinocyst stratigraphy of the Upper Miocene and lowermost Pliocene, ODP Leg 105, Site 646, Labrador Sea. In *Proceedings Ocean Drilling Project, Scientific Results, vol. 105*(eds S. P. Srivastava, M. A. Arthur & B. Clement), pp. 423–51. College Station, Texas.

HEAD, M. J., NORRIS, G. & MUDIE, P. 1989*b*. New species of dinoflagellate cysts and a new species of acritarch from the Upper Miocene and lowermost Pliocene, ODP Leg 105, Site 646, Labrador Sea. In *Proceedings Ocean Drilling Project, Scientific Results, vol. 105* (eds S. P. Srivastava, M. A. Arthur & B. Clement), pp. 453–66. College Station, Texas.

HEAD, M. J., NORRIS, G. & MUDIE, P. 1989*c*. Palynology and dinocyst stratigraphy of the Miocene in ODP Leg 105, Hole 645E, Baffin Bay. In *Proceedings Ocean Drilling Program, Scientific Results, vol. 105* (eds S. P. Srivastava, M. A. Arthur & B. Clement), pp. 467–514. College Station, Texas.

HENRIET, J. P., DE MOL, B., PILLEN, S., VANNESTE, M., VAN ROOIJ, D., VERSTEEG, W., CROKER, P. F., SHANNON, P. M., UNNITHAN, V., BOURIAK, S. & CHACHKINE, P. 1998. Gas hydrate crystals may help build reefs. *Nature* **391**, 648–9.

HOVLAND, M., CROKER, P. F. & MARTIN, M. 1994. Fault-associated seabed mounds (carbonate knolls?) off western Ireland and north-west Australia. *Marine and Petroleum Geology* **11**(2), 232–46.

HUVENNE, V. A. I., CROKER, P. F. & HENRIET, J. P. 2002. A refreshing 3-dimensional view of an ancient sediment collapse and slope failure. *Terra Nova* **14**, 33–40.

JOHN, C. M., KARNER, G. D. & MUTTI, M. 2004. Delta O-18 and Marion Plateau backstripping: Combining two approaches to constrain late middle Miocene eustatic amplitude. *Geology* **32**(9), 829–32.

KANO, A., FERDELMAN, T. G., WILLIAMS, T., HENRIET, J.-P., ISHIKAWA, T., KAWAGOE, N., TAKASHIMA, C., KAKIZAKI, Y., ABE, K., SAKAI, S., BROWNING, E. L., LI, X. & INTEGRATED OCEAN DRILLING PROGRAM EXPEDITION 307 SCIENTISTS. 2007. Age constraints on the origin and growth history of a deep-water coral mound in the northeast Atlantic drilled during Integrated

Ocean Drilling Program Expedition 307. *Geology* **35**, 1051–4.

KIRSCHVINK, J. L. 1980. The least-square line and plane and the analysis of paleomagnetic data. *Geophysical Journal of the Royal Astronomical Society* **62**, 699–718.

LE DANOIS, E. 1948. *Les profondeurs de la mer*. Paris: Payot, 303 pp.

LOURENS, L., HILGENS, F., SHACKLETON, N. J., LASKAR, J. & WILSON, J. 2005. The Neogene. In *A Geologic Timescale 2004* (eds F. M. Gradstein, J. G. Ogg & A. G. Smith), pp. 409–30. Cambridge: Cambridge University Press.

LOUWYE, S. 2002. Dinoflagellate cyst biostratigraphy of the Upper Miocene Deurne Sands (Diest Formation) of northern Belgium, southern North Sea Basin. *Geological Journal* **37**(1), 55–67.

LOUWYE, S. 2005. The Early and Middle Miocene transgression at the southern border of the North Sea Basin (northern Belgium). *Geological Journal* **40**(4), 441–56.

LOUWYE, S., DE CONINCK, J. & VERNIERS, J. 2000. Shallow marine Lower and Middle Miocene deposits at the southern margin of the North Sea Basin: dinoflagellate cyst biostratigraphy and depositional history. *Geological Magazine* **137**, 381–94.

LOUWYE, S., HEAD, M. J. & DE SCHEPPER, S. 2004. Dinoflagellate cyst stratigraphy and palaeoecology of the Pliocene in northern Belgium, southern North Sea Basin. *Geological Magazine* **141**, 353–78.

MANUM, S. B. 1976. Dinocysts in tertiary Nowegian–Greenland Sea sediments (Deep Sea Drilling project leg 38), with observations on palynomorphs and palynodebris in relation to environment. In *Initial Reports of the Deep Sea Drilling Project, vol. 38* (eds M. Talwani & G. Udintsev), pp. 897–919. Washington D.C.: U.S. Government Printing Office.

MANUM, S. B., BOULTER, M. C., GUNNARSDOTTIR, H., RANGNES, K. & SCHOLZE, A. 1989. Eocene to Miocene palynology of the Norwegian Sea (ODP Leg 104). In *Proceedings of the Ocean Drilling Program, Scientific Results, vol. 104* (eds O. Eldholm, J. Thiede & E. Taylor), pp. 611–62. College Station, Texas.

MARRET, F. & ZONNEVELD, K. 2003. Atlas of modern organic-walled dinoflagellate cyst distribution. *Review of Palaeobotany and Palynology* **125**, 1–200.

MCDONNELL, A. & SHANNON, P. M. 2001. Comparative Tertiary stratigraphic evolution of the Porcupine and Rockall basins. In *The Petroleum Exploration of Ireland's Offshore Basins* (eds P. M. Shannon, P. Haughton & D. Corcoran), pp. 323–44. Geological Society of London, Special Publication no. 188.

MILLER, K. G., MOUNTAIN, G. S, BROWNING, J. V., KOMINZ, M., SUGARMAN, P. J., CHRISTIE-BLICK, N., KATZ, M. E. & WRIGHT, J. D. 1998. Cenozoic global sea level, sequences, and the New Jersey transect: Results from coastal plain and continental slope drilling. *Reviews of Geophysics* **36**(4), 569–601.

MILLER, K. G., WRIGHT, J. D. & FAIRBANKS, R. G. 1991. Unlocking the Ice House: Oligocene–Miocene Oxygen isotopes, Eustasy and margin erosion. *Journal of Geophysical Research* **96**, B4, 6829–48.

MOORE, J. G. & SHANNON, P. M. 1992. Palaeocene–Eocene deltaic sedimentation, Porcupine Basin, offshore Ireland – a sequence stratigraphic approach. *First Break* **10**(12), 461–9.

MUNSTERMAN, D. K. & BRINKHUIS, H. 2004. A southern North Sea Miocene dinoflagellate cyst zonation. *Netherlands Journal of Geosciences–Geologie en Mijnbouw* **83**(4), 267–85.

NAYLOR, D. & SHANNON, P. M. 1982. *The Geology of Offshore Ireland and West Britain*. London: Graham & Trotman Ltd, 161 pp.

PEARSON, I. & JENKINS, D. G. 1986. Unconformities in the Cenozoic of the North-East Atlantic. In *North Atlantic Palaeoceanography* (eds C. P. Summerhayes & N. J. Shackleton), pp. 79–86. Geological Society of London, Special Publication no. 21.

PIASECKI, S. 1980. Dinoflagellate cyst stratigraphy of the Miocene Hodde and Gram Formations, Denmark. *Bulletin of the Geological Society of Denmark* **29**, 53–76.

PIASECKI, S. 2003. Neogene dinoflagellate cysts from Davis Strait, offshore West Greenland. *Marine and Petroleum Geology* **20**(9), 1075–88.

REICHART, G. J. & BRINKHUIS, H. 2003. Late quaternary Protoperidinium cysts as indicators of paleoproductivity in the northern Arabian Sea. *Marine Micropaleontology* **49**(4), 303–15.

RICE, A. L., BILLET, D. S. M., THURSTON, M. H. & LAMPITT, R. S. 1991. The Institute of Oceanographic Sciences Biology programme in the Porcupine Seabight: background and general introduction. *Journal of the Marine Biological Association of the United Kingdom* **71**, 281–310.

SHANNON, P. M. 1991. The development of Irish offshore sedimentary basins. *Journal of the Geological Society, London* **148**, 181–9.

SHEVENELL, A. E., KENNETT, J. P. & LEA, D. W. 2004. Middle Miocene Southern Ocean cooling and Antarctic cryosphere expansion. *Science* **305**, 1766–70.

STOKER, M. S., HOULT, R. J., NIELSEN, T., HJELSTUEN, B. O., LABERG, J. S., SHANNON, P. M., PRAEG, D., MATHIESEN, A., VAN WEERING, T. C. E. & MCDONNELL, A. 2005. Sedimentary and oceanographic responses to early Neogene compression on the NW European margin. *Marine and Petroleum Geology* **22**(9–10), 1031–44.

STOKER, M. S., VAN WEERING, T. C. E. & SVAERDBORG, T. 2001. A mid- to late Cenozoic tectonostratigraphic framework for the Rockall Trough. In *Petroleum Exploration of Ireland's offshore basins* (eds P. M. Shannon, P. Haughton & D. Corcoran), pp. 411–38. Geological Society of London, Special Publication no. 188.

STRAUSS, C., LUND, J. J. & LUND-CHRISTENSEN, J. 2001. Miocene dinoflagellate cyst biostratigraphy of the research well Nieder Ochtenhausen, NW Germany. *Geologisches Jahrbuch* **A152**, 395–447.

STURROCK, S. J. 1996. Biostratigraphy. In *Sequence Stratigraphy* (eds D. Emery & K. Myers), pp. 89–107. Oxford: Blackwell Science.

THOMSON, C. W. 1873. *The depths of the Sea*. London: MacMillan.

TRAVERSE, A. 1988. Production, dispersal, and sedimentation of spores/pollen. In *Paleopalynology* (ed. A. Traverse), pp. 375–430. Boston: Unwin Hyman.

VAN ROOIJ, D., BLAMART, D., KOZACHENKO, M. & HENRIET, J.-P. 2007. Small mounded contourite drifts associated with deep-water coral banks, Porcupine Seabight, NE Atlantic Ocean. In *Economic and Palaeoceanographic Significance of Contourite Deposits* (eds A. Viana & M.

Rebesco), pp. 225–44. Geological Society of London, Special Publication no. 276.

VAN ROOIJ, D., DE MOL, B., HUVENNE, V., IVANOV, M. K. & HENRIET, J.-P. 2003. Seismic evidence of current-controlled sedimentation in the Belgica mound province, upper Porcupine slope, southwest of Ireland. *Marine Geology* **195**, 31–53.

VERSTEEGH, G. & ZONNEVELD, K. 1994. Determination of (palaeo-)ecological preferences of dinoflagellates by applying detrended and canonical correspondence analysis to Late Pliocene dinoflagellate cyst assemblages of the south Italian Singa section. *Review of Palaeobotany and Palynology* **84**(1–2), 181–99.

VERSTEEGH, G. J. M. 1994. Recognition of cyclic and non-cyclic environmental changes in the mediterranean Pliocene: a palynological approach. *Marine Micropaleontology* **23**, 147–83.

VERSTEEGH, G. J. M., BRINKHUIS, H., VISSCHER, H. & ZONNEVELD, K. A. F. 1996. The relation between productivity and temperature in the Pliocene North Atlantic at the onset of northern hemisphere glaciation: A palynological study. *Global And Planetary Change* **11**(4), 155–65.

WARNY, S. A & WRENN, J. H. 2002. Upper Neogene dinoflagellate cyst ecostratigraphy of the Atlantic coast of Morocco. *Micropaleontology* **48**(3), 257–72.

WESTERHOLD, T., BICKERT, T. & ROHL, U. 2005. Middle to late Miocene oxygen isotope stratigraphy of ODP site 1085 (SE Atlantic): new constrains on miocene climate variability and sea-level fluctuations. *Palaeogeography, Palaeoclimatology, Palaeoecology* **217**(3–4), 205–22.

WILLIAMS, G. L., BRINKHUIS, H., PEARCE, M. A., FENSOME, R. A. & WEEGINK, J. W. 2004. Southern Ocean and global dinoflagellate cyst events compared. Index events for the Late Cretaceous–Neogene. *In Proceedings of the Ocean Drilling Program, Scientific Results, vol. 189* (eds N. F. Exon, J. P. Kennett & M. J. Malone), pp. 1–98. College Station, Texas.

ZACHOS, J., PAGANI, M., SLOAN, L., THOMAS, E. & BILLUPS, K. 2001. Trends, rhythms, and aberrations in global climate 65 Ma to present. *Science* **292**, 686–93.

ZEVENBOOM, D. 1995. *Dinoflagellate cysts from the Mediterranean Late Oligocene and Miocene. CIP-gegevens Koninklijke Bibliotheek Den Haag*, 221 pp. (published Ph.D. thesis, University of Utrecht, The Netherlands.)

ZEVENBOOM, D., BRINKHUIS, H. & VISSCHER, H. 1994. Dinoflagellate cysts palaeoenvironmental analysis of the Oligocene/Miocene transition in northwest and central Italy. *Giornale di Geologia* serie 3a **56**(1), 155–69.

ZHANG, C. & OGG, J. G. 2003. An integrated paleomagnetic analysis program for stratigraphy labs and research projects. *Computers & Geosciences* **29**, 613–25.

ZONNEVELD, K. A. F., VERSTEEGH, G. J. M. & DE LANGE, G. J. 2001. Palaeoproductivity and post-depositional aerobic organic matter decay reflected by dinoflagellate cyst assemblages of the Eastern Mediterranean S1 sapropel. *Marine Geology* **172**(3–4), 181–95.